Review

Abderrazak Traidia, Elias Chatzidouros and Mustapha Jouiad*

Review of hydrogen-assisted cracking models for application to service lifetime prediction and challenges in the oil and gas industry

https://doi.org/10.1515/corrrev-2017-0079
Received July 7, 2017; accepted January 6, 2018; previously published online February 13, 2018

Abstract: The present manuscript reviews state-of-the art models of hydrogen-assisted cracking (HAC) with potential for application to remaining life prediction of oil and gas components susceptible to various forms of hydrogen embrittlement (HE), namely, hydrogen-induced cracking (HIC), sulfide stress cracking (SSC), and HE-controlled stress corrosion cracking (SCC). Existing continuum models are compared in terms of their ability to predict the threshold stress intensity factor and crack growth rate accounting for the complex couplings between hydrogen transport and accumulation at the fracture process zone, local embrittlement, and subsequent fracture. Emerging multiscale approaches are also discussed, and studies relative to HE in metals and especially steels are presented. Finally, the challenges that hinder the application of existing models to component integrity assessment and remaining life prediction are discussed with respect to identification of model parameters and limitations of the fracture similitude, which paves the way to new directions for further research.

Keywords: hydrogen damage mechanisms; hydrogen embrittlement; integrity prognosis in oil and gas; models of hydrogen-assisted cracking.

1 Introduction

The general tendency worldwide is the increased sourness of produced oil and gas reservoirs reaching up to 20% H_2S content in some regions of the world (e.g. Kashagan field, Kazakhstan). These reservoirs, which were considered non-profitable for production, are nowadays being reconsidered owing to the growing world's energy demands. It is well known that steels used in the oil and gas industry can suffer from different forms of hydrogen embrittlement (HE), among blistering, hydrogen-induced cracking (HIC)/stress-oriented hydrogen induced cracking (SOHIC), sulfide stress cracking (SSC), and stress corrosion cracking (SCC). These types of damages can be triggered at relatively low stress levels and pose serious threat to structural integrity, thus the importance of having reliable integrity assessment and predictive models.

The main driver for the increased research around modeling of hydrogen-assisted cracking (HAC) of metals is certainly the so-called *subcritical cracking*. In the absence of hydrogen, (linear elastic) fracture mechanics (LEFM) theory predicts that a crack in a metallic component will grow when the stress intensity factor (SIF) at the crack tip reaches an "intrinsic" material property – the fracture toughness, noted K_{IC}. However, when the metal is subject to hydrogen charging (e.g. through exposure to high pressure hydrogen gas or through electrolytes), the onset of crack growth takes place at lower stress intensity (*subcritical*), known as threshold stress intensity and noted K_{TH}. Reported threshold values for high-strength steels can be as low as 5–25% of the hydrogen-free K_{IC} (Gangloff, 2003a,b). A standard subcritical fracture toughness test (ASTM E1681-03, 2003) characterizes the dependence of crack velocity (da/dt) on applied SIF (K_I) and often exhibits the well-known three-stage behavior. From a practical point of view, the important parameters obtained from such tests, which are critical for component integrity analysis, are the threshold stress intensity K_{TH} and the stage II crack growth rate $(da/dt)_{II}$. The former controls the onset of subcritical cracking, whereas the latter impacts the remaining lifetime before equipment failure. For a given alloy and hydrogen charging condition, the graph of da/dt vs. K_I will depend on (1) the alloy characteristics (strength, microstructure),

***Corresponding author: Mustapha Jouiad,** Masdar Institute of Science and Technology, A Part of Khalifa University of Science and Technology, PO Box 54224, Abu Dhabi, United Arab Emirates, e-mail: mjouiad@masdar.ac.ae
Abderrazak Traidia: Research and Development Center, Saudi Aramco, PO Box 62, Dhahran 31311, Saudi Arabia
Elias Chatzidouros: ALS Marine Consultants Ltd, PO Box 57356, CY-3315, Limassol, Cyprus

(2) environmental factors (nature and severity of the hydrogen charging environment and test temperature), and (3) the test method (loading format; fixed K, rising K, loading rate dK/dt).

Modeling the transport of hydrogen in the steels and subsequent *subcritical cracking* can have multiple benefits throughout the life chain of the metallic component; (1) during alloy manufacturing stage, (2) at the steel selection stage, and finally, (3) during normal operation for component integrity assessments. Model results can be used to better understand the dependency of HAC on metallurgical factors, which has an obvious implication on the design of hydrogen-compatible steels (Dadfarnia et al., 2012). Predicted subcritical growth parameters can also be used as additional steel selection criteria during the procurement of new equipment used in hydrogen-containing environment. Moreover, model predictions are critically needed for the assessment of remaining lifetime of safety critical components subject to HAC. Knowledge of the remaining lifetime is particularly useful for the optimization of non-destructive testing inspection frequency as well as the proactive planning for component repair and replacement. The fracture mechanics similitude (better known as K-similitude) provides the theoretical foundations to enable such lifetime predictions. The K-similitude assumes that, for a given alloy and hydrogen charging condition, the dependence of da/dt on applied K is uniquely defined, independently on crack and component geometry and load intensity. This is particularly powerful as the subcritical growth law da/dt vs. K (measured in laboratory experiments or predicted numerically via HAC models) can therefore be directly integrated into large-scale continuum models to predict structural integrity and time to failure, in the same manner with which fatigue laws (da/dt vs. ΔK) have been used for lifetime prediction over the last 50 years (Gangloff, 2003a,b). This approach has been successfully used recently for the development of *SCCrack* (Gangloff, 2016), a probabilistic lifetime prediction tool for SCC damage.

The present review will first briefly review the most established hydrogen degradation theories, which are at the basis of HAC models. In a subsequent section, a review of existing micromechanical models for HAC is proposed, with comparison of their capabilities and highlights on technical gaps. Emerging work on multiscale modeling of HAC will be discussed in detail in a separate section. Finally, the last section will summarize issues and challenges for transferability of existing models to industry and their integration into large-scale component integrity analysis tools.

2 Hydrogen degradation theories

There are several theories about the mechanism of HAC covering different scales and tackling different aspects of HE in steels (McLellan & Harkins, 1975; Hirth, 1980; Kirchheim, 1988; Magnin, 1995; Fukai, 2006; Gangloff & Somerday, 2012; Robertson et al., 2015). One of the more widely cited is that atomic hydrogen has a very high diffusion rate through the steel, combined with a low escape rate from its surface. Apparently, escape from the surface comes only from recombination at the surface with another hydrogen atom to form molecular hydrogen, which readily escapes the surface. Such recombination is supposed to take place at very small voids near grain boundaries, interstitials, and defects. This hydrogen concentration locally raises the stress in these sites, resulting in a noticeable reduction in energy-to-rupture. This can progress to the point where the energy-to-rupture is nil and a spontaneous crack occurs, leading to the steel failure.

Another important problem associated with steels in hydrogen gas service is the permeation of hydrogen through steels under pressure or stress, resulting in the degradation of the steel's mechanical properties leading to hydrogen-assisted fracture, which compromises the structural integrity of steel plants. In the following, various mechanisms of HE will be addressed and discussed.

2.1 Hydrogen pressure theory (HPT)

This theory considers that steel degradation is related to the increase of hydrogen concentration within internal voids, interstitials, or grain boundaries. Once hydrogen atoms in gaseous form saturate the inner sites, there will be a pressure build-up especially at sharp crack tips, resulting in higher internal stresses and promoting void growth and coalescence, which in turn will lead to cracks propagation. This mechanism is often related to blisters formation and coalescence, leading to increasing pressure or stress to fatal failure (Zapffe & Sims, 1941; Tetelman, 1969). However, many observations of stable crack growth in dry hydrogen gas, as well as in chlorine and other gaseous environments, show that the pressure theory is not always at the origin of fatal cracks. Indeed, it was observed that defects such as dislocations induce higher internal pressure in voids even if the source of hydrogen was at very low fugacity. Dislocations may act as pipelines to the diffusion of hydrogen atoms accelerating HAC with lower hydrogen pressure (Roberston et al., 2009; Birnbaum & Sofronis, 1994; Robertson et al., 2001). However, the theoretical predictions of the internal

pressure overestimate the arrival rate of hydrogen flows and underestimates its escape from the voids, hence the pressure buildup at the vicinity of the voids is generally overestimated.

2.2 Hydrogen-enhanced decohesion (HEDE)

The HEDE theory considers that hydrogen diffusing with a large amount into grain boundaries, interstitials, and precipitates is weakening the interatomic bonds in metals under stress leading to breakage of atomic binding to accommodate the slip (Oriani, 1972; Lynch, 2012). This mechanism was first introduced to explain, in one hand, the load relaxation during the tensile tests and, on the other hand, the intergranular failure. According to Lynch (2003), dislocations activity may occur during the decohesion, which will increase the local stresses at specific sites such as atomically sharp crack tips due to adsorbed hydrogen and at the vicinity of cracks where dislocation entanglements result in a tensile-stress maximum.

2.3 Hydrogen-enhanced localized plasticity (HELP)

Beachem (1972) was the first to introduce HELP mechanism. According to his model, the high hydrogen concentration dissolving in the lattice ahead of the crack tip assists in the deformation by dislocations and hence increases plasticity. He also considered that metal microstructure, crack tip stress intensity, and concentration of hydrogen are the key factors favoring such mechanism and influencing the failure mode such as intergranular, quasicleavage, or microvoid coalescence. More precisely, Beachem's model suggests that hydrogen does not inhibit dislocation motion by locking them but rather allows dislocations to multiply and move inside the steels at reduced stresses. Therefore, hydrogen simply permits or assists the normal fracture processes to become operative at unusually low macroscopic strains. Many experimental evidences conducted in transmission electron microscope (TEM) on various metal structures such as bcc, fcc, and hcp support the fact that the mobility of dislocations is enhanced by the presence of hydrogen (Beachem, 1972; Sirois & Birnbaum, 1992; Sofronis & Birnbaum, 1995; Ferreira et al., 1998; Chateau et al., 2002; Robertson et al., 2009).

Typically, hydrogen will diffuse at dislocations core, increasing dramatically the internal stress, which will boost the dislocations mobility and favor the planar deformation by pile-ups dislocations. The increasing number of dislocations will then apply greater stress at the head of dislocation pile-ups, leading to easy glide at lower macroscopic strains and resulting on softening phenomena observed on macroscopic tensile tests (Ferreira et al., 1998; Jouiad et al., 1998). However, it should be noted that dislocation motion's enhancement by the diffusion of hydrogen is merely a contributing factor to an overall degradation process and not a mechanism on its own. First, there should be enough plastic flow to create dislocation sites for hydrogen to diffuse and enhance the plasticity, and then the HELP mechanism will be prominent.

It is also worth noticing here that when hydrogen is adsorbed at the crack tip and/or at the voids, adsorption-induced dislocation emission (AIDE) mechanism may occur. AIDE is another complex mechanism of HE that includes both dislocations nucleation and emission, leading to more plastic deformation of the steels. HE due to AIDE is related to the action of adsorbed hydrogen, which is weakening the atomic bounds. It is always attributed to cleavage-like and/or dimpled intergranular failures where diffused hydrogen at those sites is at the origin of dislocations multiplication under stress. There will be then impinging dislocations from those failed sites acting as sources of defects emitting toward healthy material. The reader may refer to more detailed reports on these HE mechanisms in the following references (Oriani, 1972; Robertson, 2001; Lynch, 2003).

2.4 Stress-induced hydride formation

This mechanism does not concern iron and nickel alloys. Hydride-forming metals like titanium, zirconium, and vanadium suffer from hydrogen absorption, which causes severe embrittlement. Even at low hydrogen concentration, below the solid solubility limit, stress-assisted hydride formation provokes embrittlement, which is enhanced by slow straining. At higher hydrogen concentrations above the solubility limit, brittle hydrides are precipitated on slip planes and cause severe embrittlement (Pardee & Paton, 1980). This mechanism is also favored by increased strain rates, decreased temperature, and presence of notches in the tested steel. Generally applied stresses to the metal accelerate the formation of hydride. Consequently, hydride formation will recur in the stress field at the crack tip, and the crack will continue to propagate until failure (Kumnick & Johnson, 1980; Gerberich et al., 1986; Huang & Herberich, 1992; Huang & Herberich, 1994; Gerberich, 2012).

Other mechanisms of HE may also occur; however, it is most likely that there is not only one prevailing mechanism responsible for the material failure but rather a real competition between these mechanisms. As the material tends to minimize its internal energy during the failure, all mechanisms may occur simultaneously or alternatively considering the most favorable mechanism with respect to the steel configuration during the damage process, as described by Lynch (2003). According to his assumptions, the steels may undergo a combination of AIDE, HELP, and HEDE mechanisms depending on the fracture mode, which depends on the material structure and other variables such as stress concentration and sample geometry. For example, the dislocations nucleated from the crack tip and explained well via AIDE mechanism may also be explained via HELP mechanism. For both mechanisms, the dislocations movement away from the crack tip will minimize the back-stress on subsequent dislocation emission.

3 Micromechanical models of HAC

3.1 Model classification

Micromechanical modeling of HAC is a growing area of research and development. Supported by the easy availability of high-performance computing facilities, HAC models are constantly growing in complexity. Far from providing a comprehensive review of the exhaustive literature on micromechanical modeling of HAC (Gangloff, 2003a,b; Gerberich, 2012), the present article focuses on a summary and discussion of key models as well as current emerging trends that might be of benefit for the oil and gas industry.

Models of HAC are varying in complexity in terms of both mechanisms and couplings. Different criteria can be used to compare available models:

(a) crack configuration: stationary or growing crack, surface or bulk crack, remote external load (static/dynamic) and/or internal crack pressure build-up (e.g. HIC);
(b) source of hydrogen: internal or environmental, H produced at the crack surface or far from the crack surface;
(c) hydrogen diffusion: transient or steady state, unidimensional or multi-dimensional, weak or strong coupling with crack tip mechanics, concentration-driven and/or stress-driven, explicit analysis of trapping or analytical approximation, microstructure-dependent traps and/or plastic strain-dependent traps;
(d) crack tip mechanics: small deformation or finite deformation theory, linear elastic FM or elastoplastic FM, conventional plasticity (J2) or non-conventional (strain gradient plasticity, dislocation dynamics), weak or strong coupling to local H concentration, explicit stress analysis or simplified analytical solutions;
(e) failure mechanism: decohesion-based (HEDE) and/or plasticity-based (HELP) and/or hydrogen-pressure based (HPT).

Available micromechanical and continuum models for HAC are commonly grouped either by failure mechanism (HEDE versus HELP) (Gerberich, 2012) or by type of hydrogen degradation [internal hydrogen assisted cracking (IHAC) versus hydrogen environment assisted cracking (HEAC)] (Gangloff, 2003a,b). In the present review, we adopt another classification aligned with the historical development and evolution of available models: (1) unidimensional models occluding the three-dimensional (3D) distribution of hydrogen concentration and stresses (using semi-analytical approximate solutions) but with the benefit of an explicit relationship between subcritical growth indicators (i.e. K_{TH} and da/dt), steel properties (yield strength and cohesive stress, H diffusivity), and environment (i.e. H charging pressure/concentration, temperature and applied K) and (2) multidimensional models, which offer a detailed time-dependent analysis of the different chemo-mechanical couplings in the FPZ and leading to advanced two-dimensional (2D)/3D finite element (FE) models.

It is worth noticing that the most available HAC models' assumptions are based on diffusion-controlled hydrogen permeation to the FPZ. This is quite acceptable when the hydrogen degradation mechanisms occur due to a source of hydrogen far away from the FPZ (i.e. IHAC) because of the relatively large diffusion distance. Fortunately, for the HIC mechanism encountered in the oil and gas industry, which is a bulk cracking phenomenon, HAC models' assumptions fairly hold. However, for HEAC degradation (such as SCC) where the production of hydrogen happens at the crack surface, the assumption of diffusion-controlled must be carefully verified. To that extent, Turnbull et al. (1996) showed that the use of generalized boundary condition at the crack tip (based on flux and not on constant concentration) allows to properly capture the kinetics of hydrogen at the vicinity of the crack tip and subsequently predict proper crack growth rates. A similar analysis was proposed more recently by Crolet (2016). Analytical models might be quite difficult to revise with the generalized boundary condition proposed by Turnbull

et al. (1996); however, this could be introduced in multidimensional numerical models discussed later in the present review.

3.2 Unidimensional approaches to HAC modeling

Table 1 summarizes selected unidimensional models for HAC (with apologies to many authors whose work is not cited). These selected models for HAZ are all based on the decohesion mechanism (HEDE). Note that models of hydrogen diffusion only (i.e. no coupling to any specific hydrogen degradation mechanism) have not been considered.

By coupling a steady-state hydrogen decohesion model to an analytical solution of the elastoplastic stress field ahead of a stationary surface crack exposed to hydrogen pressure p_{H_2}, Akhurst and Baker (1981) proposed a simple model to predict the dependence of K_{TH} on p_{H_2}. The fundamental assumption of this model is that subcritical cracking occurs (i.e. $K_I = K_{TH}$) when the tensile stress σ_{yy}, exceeds the H-reduced cohesive stress σ^* over a cohesive ligament of length x_C. This critical ligament length x_C along which hydrogen damage nucleates is assumed to be a steel property, which is adjusted to fit predictions with experiments. Historically, this failure criterion finds its roots in the model proposed by Ritchie et al. (1973), better known as the RKR model, which was initially proposed for cleavage failure in the absence of hydrogen and used to predict the relationship between critical tensile stress at failure and the fracture toughness K_{IC}.

In the presence of hydrogen, Akhurst and Baker (1981) suggested the following relationship for the H-degraded cohesive stress ahead of the crack tip:

$$\sigma^* = \sigma_0^* - A\sqrt{p_{H_2}}\exp\left(V_H \frac{2.6\sigma_{yy} - 1.3\sigma_{ys}}{3RT}\right), \quad (1)$$

where σ_0^* is the hydrogen-free cohesive stress, A is an embrittlement factor, and V_H is the partial molar volume of hydrogen in metal. The distribution of tensile stress σ_{yy} ahead of the crack tip was taken as a function of the yield stress σ_{ys} and the hardening exponent n, assuming a conventional J2 plasticity (Schwalbe, 1977):

$$\sigma_{yy} = \sigma_{ys}\left(\frac{0.3}{X+1}\right)\left(\frac{0.04}{X}\right)^{\frac{1}{n+1}},\ 0.04 \le X = \frac{x}{(K_I/\sigma_{ys})^2} \le 0.073 \quad (2)$$

The model was used successfully to predict the decrease in K_{TH} with p_{H_2} provided that the fitting parameters A and σ_0^* and x_c are properly selected. This is certainly the main drawback of this simple model, as there is no guarantee

Table 1: Comparison of selected unidimensional models for HAC.

		Akhurst and Baker (1981)	Huang and Gerberich (1994)	Gerberich et al. (1986, 1988, 1991, 1996)	Gerberich et al. (1996, 2012)	Unger (1986, 1989, 1995)
Can predict	Threshold (K_{TH})					
	Growth rate $(da/dt)_{II}$					
Crack configuration	Stationary					
	Growing					
	Surface					
	Bulk					
H source and H diffusion	Internal hydrogen					
	Environmental hydrogen					
	Steady-state analysis					
	Transient analysis					
	Stress-driven diffusion					
	Explicit trapping analysis					
	Trapping approximation					
Crack tip mechanics	LEFM					
	EPFM					
	J2 plasticity					
	Non-conventional plasticity					
Failure mechanism	HEDE					
	HELP					
	HPT					

Gray shades mean that the testing in left side were accomplished. When the table boxes are blank, it means that the tests were not achieved.

on the uniqueness of optimum parameter set. Furthermore, the use of conventional J2 plasticity failed in predicting a sufficiently high level of stress concentration, few nanometers ahead of the crack tip, as necessary to break atomic bonds.

To address the shortcomings of conventional J2 plasticity, Huang and Gerberich (1994) and Gerberich et al. (1986) proposed a different mechanistic model, based on dislocation dynamics, which describes the dependency of threshold intensity K_{TH} on the local hydrogen concentration at the FPZ, noted $C_{H\text{-}FPZ}$. Their model was inspired by the pioneering work of Thomson and co-workers (in the absence of hydrogen) on dislocation emission and shielding at the crack tip. The proposed model gave a threshold stress intensity in the following form:

$$K_{TH} \approx \frac{1}{\beta'} \exp\left[\frac{(k_{IG} - k_{IH})^2}{\alpha' \sigma_{ys}}\right], \tag{3}$$

where k_{IG} is the "local" hydrogen-free steel fracture toughness (in the Griffith sense) expressed as function of the surface energy γ_S as $k_{IG} = \sqrt{2E\gamma_S}$, whereas k_{IH} is the local H-reduced fracture toughness varying linearly with the local hydrogen concentration at the crack tip FPZ as follows: $k_{IH} = \alpha C_{H\text{-}FPZ}$. For aqueous hydrogen charging, Gangloff (2003a,b, 2008) suggested the following expression for the hydrogen accumulation at the crack tip FPZ:

$$C_{H\text{-}FPZ} = C_S \exp\left(\frac{E_B + \sigma_H V_H}{RT}\right), \tag{4}$$

where C_S is the hydrogen concertation at the crack surface, σ_H is the local hydrostatic stress, and E_B is the trap binding energy. The values of the other model parameters used in Equation 3 (i.e. α, α' and β') were determined from computer simulations. Gerberich et al. (1996) reported good model predictions with respect to experiments carried out on high-strength steels when using $\alpha = 0.5$ MPa $\cdot$ m$^{1/2}$/atom fraction, $\alpha' = 2 \times 10^{-4}$ MPa $\cdot$ m and $1/\beta' = 5$ MPa $\cdot$ m$^{1/2}$. Not only that this model allowed to address theoretically the deficiency of conventional continuum EPFM in predicting high stress levels in the close proximity of the crack tip (in this model, predicted hydrostatic stress can reach up to 50 times σ_{ys}), but also, it explained the correlation observed experimentally between the threshold stress intensity K_{TH} and the hydrogen-free fracture toughness K_{IC} in high-strength steels [note that in Equation 3, $K_{IC} = K_{TH}(C_H = 0)$], as well discussed by Gerberich et al. (1996).

As it pertains to predicting stage II crack growth rate, most unidimensional models rely on a simple ingredient – coupling a transient unidimensional diffusion analysis along the cohesive ligament ahead of the crack tip to a local failure criterion (often base on HEDE). Crack growth is assumed to take place when the opening stress over the critical of length x_c exceeds the material cohesive stress (Van Leeuwen, 1979; Gerberich et al., 1986, 1988, 1991, 1996; Chen & Gerberich, 1991; Toribio & Kharin, 1997; Hall and Symons, 2001). The unidimensional diffusion analysis is used to determine the critical time t_c for hydrogen to diffuse from C_S at the crack surface over the critical distance x_c to reach a critical hydrogen concentration C_{CRIT} in the FPZ. Stage II growth rate is then simply derived as the ratio x_c/t_c. In other words, subcritical crack growth is assumed to take place in the form of successive (instantaneous) crack jumps of length x_c with a period between successive jumps being t_c. Hydrogen equilibrium on the newly created crack surface is assumed to take place immediately upon the crack jump, and therefore, a constant hydrogen concentration C_S is prescribed as a boundary condition at the newly created crack surfaces. Note that we have limited the present review to growth rate models where hydrogen diffusivity is the rate-limiting step for crack growth. This assumption is valid for internal hydrogen embrittlement (IHAC); however, it may not hold for environment hydrogen embrittlement (HEAC), as extensively discussed by Gangloff (2003a,b).

Gangloff (2003a,b, 2008) proposed a generalized formalism encompassing the most available diffusion-controlled models for stage II growth rate, as follows:

$$\left(\frac{da}{dt}\right)_{II} = \frac{D_{Heff}}{x_c}\left[\xi\left(\frac{C_S}{C_{CRIT}}, D_H, x_c, \sigma_{ys}, t\right)\right], \tag{5}$$

where D_{Heff} is the effective (trapping) hydrogen diffusion coefficient, and ξ is a function of the above-indicated variables giving an output from 0.01 to 4, depending on the model. Note that in order to provide a valid formalism for both IHAC and HEAC, Gerberich et al. (1996) replaced the factor $\frac{1}{x_c}$ by $\frac{x_a}{x_d^2}$, where x_a is the elementary crack advance and x_d is the diffusion distance (i.e. the average distance travelled by hydrogen to accumulate in the FPZ), which equals x_a in the case of HEAC (and reduces to Equation 5 with $x_a = x_c$).

Extensive HEAC experiments carried out by Gangloff (2003a,b) at the University of Virginia showed that the fastest measured stage II crack growth rats $(da/dt)_{II}$ correlate (almost linearly) with the best available measured values of trapped hydrogen diffusivity D_{Heff} for a wide variety of high-strength steels tested in both aqueous (chloride solutions) as well as gaseous (H_2 and H_2S) environments (see Figure 1). This important finding not only supported the assumption of diffusion control but

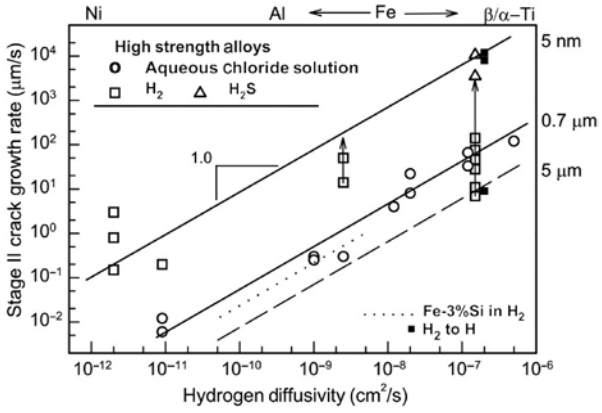

Figure 1: The dependence of $(da/dt)_{II}$ on D_{Heff} for high-strength alloys that exhibit HEAC in gases and electrolytes at 250°C. High-strength austenitic stainless steel and nickel superalloys were cracked in high pressure (100–200 MPa) H_2, while maraging and tempered-martensitic steels were cracked in low pressure (~100 kPa) H_2. The dotted line represents TG cracking of Fe-3%Si single crystal in 100 kPa H_2 at 0–125°C. Filled symbols (■) represent the transition from molecular to atomic hydrogen gas. Reprinted from Gangloff (2003a,b), with permission from Elsevier.

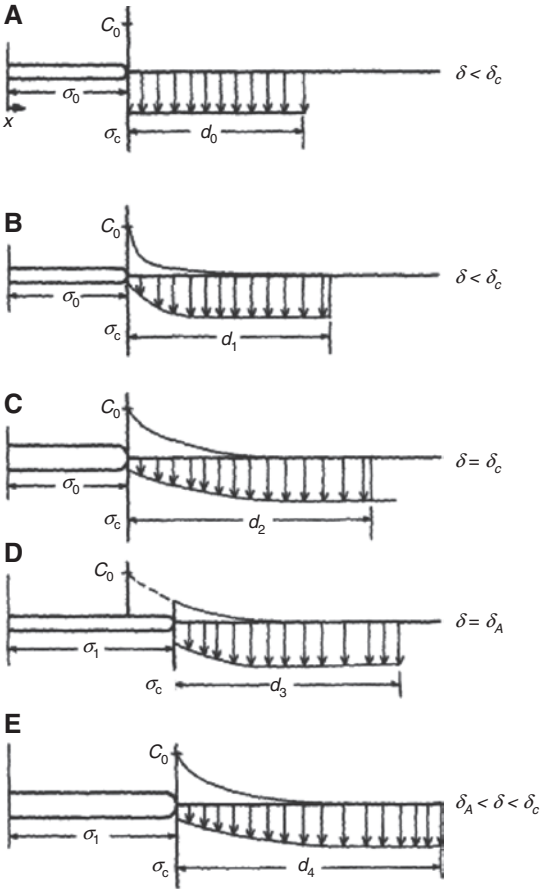

Figure 2: Crack propagation sequence as per the model proposed by Unger (1989). Reprinted from Unger (1989), with permission from Elsevier. The labels A–E represent the steps of the crack opening.

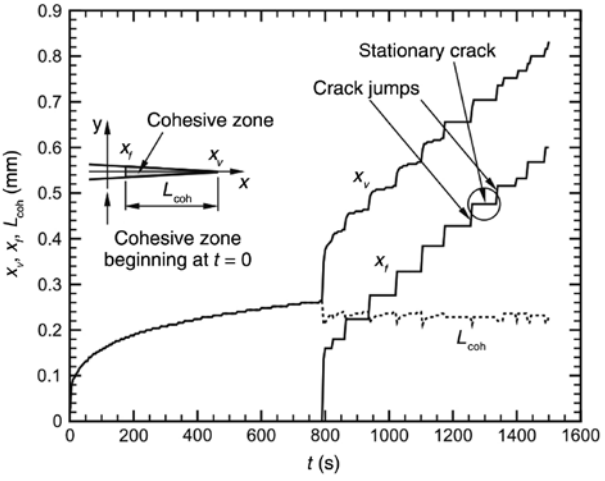

Figure 3: Typical calculated crack advancement with time using the cohesive model by Serebrinsky et al. (2004). $L_{coh} = x_v - x_f$ denotes the length of the cohesive zone. x_f Locates the traction-free point, behind which the crack flanks experience zero traction. x_v Locates the vertex of the cohesive zone, ahead of which there is zero opening displacement. Reprinted from Serebrinsky et al. (2004), with permission from Elsevier.

also provided a mean for estimating the critical "steel" parameter x_c. Using the crack growth rate measurements shown in Figure 2, Gangloff suggested that ξ shall not exceed 3, which yields to $x_c = 0.7$ μm.

Using a different approach, Neimitz and Aifantis (1985, 1987a,b) proposed an incremental subcritical growth model based on a Barenblatt cohesive zone (ahead of a growing crack) that degrades with time due to the accumulation of hydrogen in the FPZ. Almost in parallel, Unger (1989) proposed an incremental HAC model using a Barenblatt/Dugdale cohesive zone approach similar to that proposed by Neimitz and Aifantis (1985, 1987a,b). Unger's model, however, introduced a pointwise degradation of the cohesive force $\sigma^*(x, t)$ ahead of the crack tip by assuming a linear decrease with the local hydrogen concentration $(\sigma^*(x, t) = \sigma_0^* - \gamma C(x, t))$, which necessitated a numerical resolution of the transient coupled chemo-mechanical problem. In a subsequent work, Lee and Unger (1988) and Unger (1989) proposed a simplified (analytical) solution to the problem by assuming that the extent of the cohesive zone is small compared to the crack length. Note, however, that Unger's model used a hydrogen-free critical crack-tip opening displacement (CTOD), in contrast to the model proposed earlier by Neimitz and Aifantis (1985, 1987a,b). Figure 3 illustrates schematically the incremental model proposed by Lee and Unger (1988). Initially (a), a constant hydrogen concentration C_0 is prescribed at the crack tip located at $x = a_0$ and a remote mode I opening stress σ_∞ is applied, such that the resulting CTOD δ is

below the critical CTOD δ_c (or, equivalently, $K_I < K_{IC}$). With increasing hydrogen accumulation in the FPZ over time (b), the cohesive stress is locally reduced, which is compensated by an increase in the cohesive zone length, thus increasing the crack opening δ. When the degradation is sufficient (c) to increase δ to its critical value δ_c (assumed to be independent of H content), crack extension occurs and is accompanied by a drop in δ due to the sudden increase of the cohesive stress ahead of the newly created crack front as it enters the healthy portion of the steel. Crack will arrest (d) when most of the hydrogen damage zone has passed and the material ahead the new crack tip is essentially healthy. The crack opening δ drops then to an equilibrium value $\delta_A < \delta_c$. The hydrogen concentration at the newly created crack tip ($x = a_1$) is then fixed to C_0 (e), assuming fast equilibrium takes place immediately after the crack jump. The cycle (e)-(c)-(d)-(e) continues over time causing incremental crack jumps until the length of the crack reaches a critical value where $\delta = \delta_c$ even in the absence of hydrogen ($C_0 = 0$) and unstable failure takes place. This incremental model successfully captured the characteristic three-stage curve of da/dt vs. K using γC_0 as the only fitting parameter. Unger (1995) proposed some insights on how to identify this parameter from standard threshold stress intensity laboratory measurements. The main limitation of this model is the absence of hydrogen trapping as well as the absence of plasticity effects. This necessitates the use of a FE approach as described in the next section.

3.3 Multidimensional approaches to HAC modeling

Selected multidimensional models suitable for the prediction of threshold stress intensity and/or subcritical HAC growth rates are presented in Table 2. The literature review clearly shows that the cohesive zone modeling (CZM) approach has been extensively used over the last decade in HAC modeling. This method, initially introduced by Needleman (1987) to study particle matrix decohesion (in the absence of hydrogen), is particularly well adapted to decohesion/delamination type of failure and has gained popularity for being implemented in most commercial FEM packages (e.g. ABAQUS, ANSYS, COMSOL). In few words, CZM consists of introducing "interface elements" in a thin strip zone of zero (negligible) thickness aligned along the (a-priori known) crack path. Upon applying an external load, interface elements start to separate following a pre-defined relationship called traction-separation law (TSL), which relates the amount of local separation/opening δ to the local cohesive stress in the element σ^*. Complete separation at the interface occurs when a critical opening δ_c has been reached. A total energy E^* is dissipated locally during the separation process, which corresponds to the work of separation: $E^* = \int_0^{\delta_c} \sigma^*(s)\, ds$. The main advantage of CZM is its ability to separate the bulk ("global") steel behavior (as described by the macroscopic stress-strain curve) from the "local" behavior of the cohesive interface (as described by the TSL) while maintaining a clean coupling between both behaviors in a continuum fashion. This makes CZM particularly attractive for HAC modeling, as it provides the localized environment ahead of the crack tip where HE mostly takes place. In addition, the decorrelation between the local and global steel behaviors offered by CZM is quite suitable to capture the local hydrogen effect on atomic bonding energy in the FPZ independently of its impact far from the FPZ (i.e. on the plastic behavior of the bulk steel).

Serebrinsky et al. (2004) introduced a quite comprehensive continuum model for HAC to simulate brittle decohesion in bcc iron systems using quantum-based cohesive elements. The proposed model considers a strong and time-dependent coupling between hydrogen transport and the local degradation of the cohesive zone ahead of a growing crack. The hydrogen transport in the pre-cracked continuum was described by a stress-driven Fickian diffusion (neglecting explicitly trapped hydrogen concentration) as follows:

$$\frac{\partial C}{\partial t} = D\nabla^2 C - \frac{DV_H}{RT}\nabla C \cdot \nabla \sigma_H - \frac{DV_H}{RT} C \nabla^2 \sigma_H, \tag{6}$$

where V_H is the partial molar volume of hydrogen in the metal solid solution and σ_H is the hydrostatic stress ($-\sigma_{ii}/3$). The effect of trap sites on hydrogen diffusion was implicitly considered through an effective diffusivity coefficient (D_{Heff}). The value of the hydrostatic stress was derived from a static stress analysis assuming a conventional J2 elastoplastic steel behavior with power law strain hardening. Crack extension was driven by brittle decohesion along {110} planes and was modeled by cohesive elements with a linear hydrogen-affected TSL, fully described by two parameters: the critical cohesive stress σ_c^* and critical opening δ_c. The dependence of the surface energy (ideal work of fracture) on local hydrogen coverage θ was derived from first principles *ab initio* simulations carried out by Jiang and Carter (2004). Assuming that the critical opening δ_c is insensitive to hydrogen coverage, the critical cohesive stress decreases with hydrogen coverage following the same dependency as the surface energy presented

Table 2: Comparison of selected multidimensional models for HAC.

		Serebrinsky et al. (2004)	Ahn et al. (2007a,b)	Olden et al. (2007, 2008a,b, 2009a,b, 2012)	Dadfarnia et al. (2009, 2012)	Dadfarnia et al. (2014)
Can predict	Embrittlement (K_{TH} or TSL)	■	■	■	■	■
	Growth rate (da/dt)					
Crack configurationn	Stationary	■	■	■	■	■
	Growing					
	Surface					
	Bulk					
H source and H diffusion	Internal hydrogen	■	■	■	■	■
	Environmental hydrogen					
	Steady-state analysis	■	■	■	■	■
	Transient analysis					
	Stress-driven diffusion					
	Microstructural traps					
	Plasticity-dependent traps					
	Explicit trapping analysis					
	Trapping approximation	■		■		
Crack tip mechanics	LEFM	■	■	■	■	■
	EPFM					
	J2 plasticity					
	Non-conventional plasticity					
	Cohesive zone model (CZM)	■	■	■	■	
	Node release approach					■
Failure mechanism	HEDE	■	■	■	■	■
	HELP					
	HPT					

Gray shades mean that the testing in left side were accomplished. When the table boxes are blank, it means that the tests were not achieved.

in Equation 7. The hydrogen coverage θ was related to the bulk hydrogen centration C using Langmuir-Mc Lean isotherm.

$$\sigma_c^*(\theta) = (1 - 1.0467\theta + 0.1687\theta^2)\sigma_c^*(0) \tag{7}$$

The model could capture qualitatively and quantitatively stage I and II subcritical growth rates on AISI 4340 steel tested in different aqueous environments. The model results also show some interesting findings, namely, the finite crack jump at initiation (i.e. when $K_I = K_{TH}$) as well as the intermittent stepwise-like crack growth (in the order of 40-µm jumps), as shown in Figure 3. This important finding not only supports diffusion control crack growth assumption but is also in agreement with earlier results (discussed in the previous section) regarding the existence of a critical length scale x_c, which identifies to the discrete crack jump in HEAC. Furthermore, the model could reproduce the dependence of threshold stress intensity and stage II crack growth rate on environment, temperature, and yield strength.

Olden and co-workers used the model proposed by Serebrinsky et al. (2004) to simulate HEAC of 25% Cr duplex stainless steels in aqueous environment (Olden et al., 2007, 2009a,b) and more recently (in 3D) for API-5L-X70 steel welds (Olden et al., 2012; Alvaro et al., 2014). To account for the ductile failure in this class of lower strength steels, the authors introduced a polynomial traction separation law as follows:

$$\sigma^*(\delta, \theta) = \frac{27}{4}\sigma_c^*(\theta)\frac{\delta}{\delta_c}\left(1 - \frac{\delta}{\delta_c}\right)^2 \text{ for } \delta < \delta_c, \text{ otherwise } 0 \tag{8}$$

The interesting novelty in the work of Olden's group is that the hydrogen coverage θ was calculated from the "total" bulk hydrogen concentration, i.e. the sum of the lattice hydrogen concentration C_L (as computed from the stress-driven diffusion analysis) and the trapped hydrogen concentration C_T. By fitting numerical results reported by Taha and Sofronis (2001) on hydrogen transport in the vicinity of crack tip, Olden et al. (2007) overcome the cumbersome resolution of an explicit hydrogen trapping problem and proposed the following linear relationship that correlates the trapped hydrogen concentration C_T to the local cumulative plastic strain ε_p and lattice concentration C_L:

$$C_T = (49\varepsilon_p + 0.1)C_L \quad (9)$$

If the parameters of the TSL (i.e. the initial critical cohesive stress $\sigma_c^*(0)$ and the critical opening at separation δ_c) as well as the effective hydrogen diffusivity are well selected, Olden et al.'s (2007) model can properly capture the incubation time to failure, threshold stress intensity, and subcritical growth rates. For 25% Cr duplex stainless steel, Olden et al. (2007) suggested an initial critical cohesive stress in the order of $3.5\sigma_{ys}$ and a critical opening in the order of 20 μm, while for X70 steel (base metal), the proposed values are, respectively, $3.1\sigma_{ys}$ and 0.3 mm. The proposed values resulted in cohesive energies very close to experimental values derived from conventional *J-R* testing.

To reconcile HEDE and HELP in a unified model and linking the physical mechanisms of HE at the microscale to observable/measurable macroscopic quantities, Sofronis and co-workers introduced the concept of a unit cell model. Liang and Sofronis (2003) proposed a first phenomenological model to study the effect of hydrogen on void nucleation and debonding at the interface of an elastic inclusion embedded in an elastoplastic matrix. The aim of this model was to characterize the effect of hydrogen on the cohesive interface properties and its impact on the macroscopic stress at the onset of decohesion. The phenomenological approach consisted of coupling a transient model for hydrogen transport [accounting explicitly for trapped hydrogen using the trapping model proposed by Sofronis and McMeeking (1989), later modified by Krom et al. (1999)] to material deformation (local softening in the presence of hydrogen) and interfacial decohesion (reduction in the cohesive stress).

To account for the hydrogen-induced shear localization (HELP) and local softening of the elastoplastic matrix in the presence of hydrogen, which is modeled at the continuum scale through a reduction in the local flow stress σ_Y, Liang and Sofronis (2003) used the following relationship developed by the same authors in an earlier work of Sofronis et al. (2001):

$$\sigma_Y(\varepsilon_p, C) = \sigma_{Y0}(C)F_p(\varepsilon_p) \quad (10)$$

where C is the local total hydrogen concentration (lattice and trapped), F_p is the strain hardening function (taken as a power law of the cumulative plastic deformation ε_p), and $\sigma_{Y0}(C)$ is the yield stress in the presence of hydrogen. The latter is taken as a decreasing function of the local hydrogen concentration as follows:

$$\sigma_{Y0}(C) = [(\xi - 1)C + 1]\sigma_{Y0} \quad (11)$$

where σ_{Y0} is the hydrogen-free yield stress and $\xi \leq 1$ is a softening factor.

To account for interfacial decohesion at the inclusion/matrix boundary, cohesive FEs were introduced at this interface. The authors used a 2D polynomial TSL (in the sense that both normal and tangential openings were considered) with three parameters δ_n, δ_t and $\sigma_c^*(\Gamma)$ being, respectively, the critical normal opening (in pure normal opening mode), the critical tangential opening (in pure tangential opening mode), and the critical cohesive stress in the presence of surface segregated hydrogen at surface concentration Γ. The cohesive model parameters were then calibrated such that the reversible work of separation is exactly the same as that given by the thermodynamic interfacial decohesion model (in the presence of impurities) proposed by Hirth and Rice (1980) and Rice and Wang (1989). Full details on the model calibration procedure are given by Taha and Sofronis (2001).

In a subsequent work by Liang and Sofronis (2004), the authors introduced another complexity to their original model by adding the effect of grain boundary decohesion. The model was essentially the same – a unit cell system comprising an elastic inclusion embedded in a ductile matrix with a grain boundary passing at the axis of symmetry and loaded in the direction normal to the grain boundary plane. The model was used to simulate intergranular cracking of alloy 690. The simulation results indicated that embrittlement is essentially controlled by the hydrogen-enhanced debonding at the carbide/matrix interface, whereas the effect of hydrogen in the grain boundary decohesion was found to be almost insignificant. Furthermore, the model gave means to estimate the fracture energy at crack initiation in the presence of hydrogen.

The unit cell model was also used by Liang et al. (2004, 2008) to study the influence of hydrogen on void growth during ductile failure. In this study, the model was essentially the same as that used for void nucleation at second phase interface, except that in the study by Liang et al. (2004, 2008), no cohesive elements were used as decohesion along grain boundaries was not considered. The authors simulated the stress distribution in a unit cell comprising a spherical void in a hydrogen-softened elastoplastic matrix, loaded under a remote tensile stress. The main target was to assess the effect of hydrogen on the macroscopic (homogenized) response of the cell as described by the stress-strain curve during ductile failure. The main result was that hydrogen assists void growth regardless of the intensity of trapping and material softening but with some dependency to the stress triaxiality. The main gap filled by the unit void cell model was to provide the theoretical foundations to bridge two scales, i.e. the microstructural degradation and the macroscopic

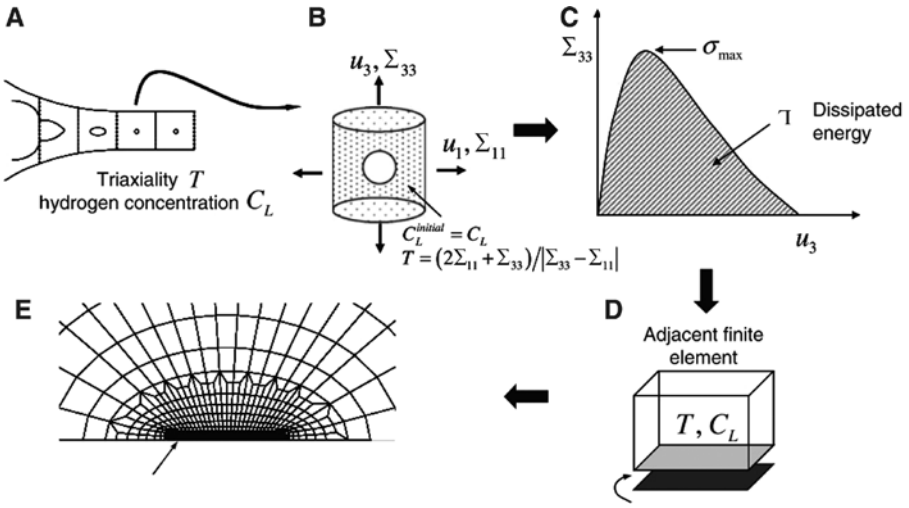

Figure 4: Two-scale modeling of hydrogen-assisted ductile crack propagation proposed by Ahn et al. (2007a,b). (A) Crack tip fracture process zone. (B) Axisymmetric void cell model. (C) Traction-separation law. (D) Cohesive element. (E) Cohesive elements characterized by a traction-separation law based on the void cell model. Reprinted from Ahn et al. (2007a,b), with permission from Springer.

observed embrittlement. As shown in Figure 4, the main idea is that phenomenological traction separation laws issued from a unit cell model can be directly integrated into a larger macroscale model of subcritical crack growth. This has been achieved by Ahn et al. (2007a,b) and successfully used to predict subcritical ductile failure in A533B pressure vessel steel.

Note that recent investigations by Dadfarnia et al. (ASTM E1681-03, 2003; Dadfarnia et al., 2009, 2014) raised questions around the fidelity and accuracy of HAC results issued from cohesive zone modeling simulations. The authors observed that crack growth required a continuously increasing FPZ and associated computed crack growth velocities were, in general, slower than those observed experimentally. In addition, the method was found not to preserve the accuracy and fidelity of hydrogen concentration and stress fields very close to the crack tip. These challenges led Dadfarnia et al. (2014) to propose a model based on the standard node release technique and the RKR (Gerberich et al., 1986) failure criterion discussed in the previous section.

4 Towards multiscale models of HAC

Multiscale modeling in solid materials refers to the numerical or computational scheme whereby multiple modeling techniques are used, each one acting at different length scale (e.g. molecular dynamics (MD) acting in nm scale, continuum mechanics (CM) acting in mm→m size) (Figure 5), to accurately portray an engineering problem. The need for multiscale modeling arises either from insufficient or poor prediction performance of available macroscale models, e.g. CM-based finite element method (FEM) or when certain types of engineering problems involve phenomena acting in smaller length scales. In this sense, the different modeling techniques acting in different length scales, although governed by different physical laws, are used together in order to acquire more accurate physics of the studied problem by modeling the phenomenon, compute properties and cause-effect relations, and transfer the necessary parameters from the lower to the

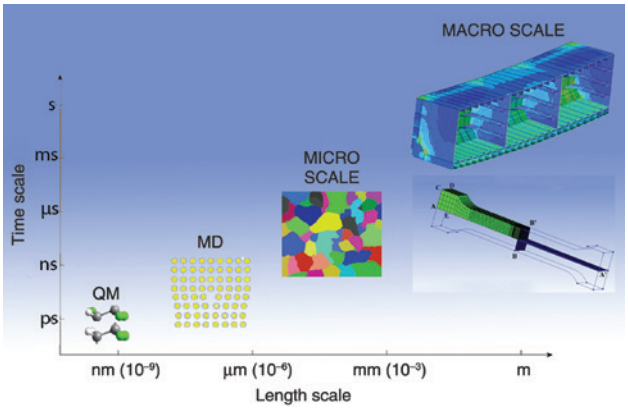

Figure 5: Multiscale modeling scheme: (A) at the smaller length scale, QM is at play, which can simulate up to a few 100 atoms; (B) MD, which can simulate millions of atoms; (C) illustrating microscale representative volume element (RVE) of a few grains of a polycrystalline material; and (A) macroscale illustrating the models of tension specimen and a three-compartment model of a ship.

higher scale (Jiang & Carter, 2004). Here, the numerical models are bridged together through a multiscale bridging technique, which is either sequential or concurrent (Jiang & Carter, 2004). Concurrent means that the parameters and/or quantities needed to solve the macroscale model are computed from the microscale during computational operations. Sequential means that when microscale parameters are needed for the macroscale model, they are precomputed from models at lower length scale, then they are integrated in the macroscale model through, e.g. statistical analysis methods, homogenization techniques, etc.

Hydrogen-related degradation phenomena are an engineering problem that has been tackled by many researchers using multiscale modeling (Zhong et al., 2000; Jiang & Carter, 2004; Horstemeyer, 2009; Counts et al., 2010; Johnson & Carter, 2010; Counts et al., 2011; Yamaguchi et al., 2011; Itakura et al., 2013; Momida et al., 2013; Matsumoto et al., 2014; Von Appen et al., 2014; Alvaro et al., 2015). The very nature of hydrogen-related damage mechanisms, as described in previous sections, has pushed forth not only academia but also industry to use multiscale modeling techniques to accurately describe the underlying physics of the problem. A more important parameter is the complexity of hydrogen degradation phenomena and its implications to many industrial sectors, such as automotive, aerospace, oil and gas pipelines, etc. Specifically, the most intriguing and demanding problem, in terms of understanding and prediction, is the structural behavior of defects cracks in the presence of hydrogen. The presence of hydrogen in front of the crack tip presents a multi-facet engineering problem, which involves hydrogen transport, interaction with iron, and also segregation at impurities and trapping in reversible or irreversible trapping sites. Furthermore, the very nature of a crack tip, an area that exhibits a high density of trapping sites (voids, dislocations, etc.), constitutes a problem that should be tackled at the microscale. There is a wide range of analytical and FE models that aim to address hydrogen-assisted behavior in front of a crack tip, based on CM and using established elasto-plastic fracture mechanic theories and, many times, damage models, which associate damage parameters with hydrogen degradation. In this context, these methods describe the interaction between crack tip stress and strain and hydrogen within the process zone (crack tip) in a phenomenological basis only.

4.1 First principles approach

In a multiscale computational framework, *ab initio* is the most basic and proper way in which the treatment of phenomena such as bond-breaking, charge transfer, electronic and optical excitations, etc. can be tackled. This can be accomplished using quantum mechanics (QM), which, owing to its high computational demand, application should be restricted to a relatively small system of a few 100 atoms. In QM computational schemes, the properties of many electron system can be properly addressed by using density functional theory (DFT), most notably in most cases, the Kohn and Sham (1965) DFT. This fact obviously restricts the augmentation of the physical problem at a small number of atoms, which calls for pairing the QM method with molecular mechanics (MM) methods, which, although empirical in nature, offer the capability of describing elastic deformations, small-amplitude vibrations, etc. The MM methods can tackle millions of atoms or more, therefore offering significant advantage over employing single QM computational schemes. A noteworthy example of empirical potential for the MM method is the embedded-atom method (EAM). Therefore, computational schemes that combine QM and MM methods offer promising solutions to challenging problems requiring atomistic simulations of materials (Lin & Truhlar, 2006; Bermstein et al., 2009; Zhang et al., 2012). In this context and employing coupled DFT and EAM potentials, Lu and Kaxiras (2004) and Choly et al. (2005) studied a different dislocation behavior (Figure 6).

Many works have been performed using first-principles approach to model hydrogen effect on Fe systems. For the first time, the reduction of cohesive energy in iron grain boundaries was reported by Zhong et al. (2000), using first-principles calculations. Other works (Tateyama & Ohno, 2003; Lu and Kaxiras, 2005) that are based on first-principles approach study the vacancy-hydrogen interactions and correlate the findings with HE. In a more recent first-principles study, Yamaguchi et al. (2011) argued that cohesive energy of bcc Fe Σ3(111) and fcc Al Σ5(012) grain boundaries can be significantly reduced if a large amount of hydrogen atoms segregate in those grain boundaries. Whereas in the study by Yamaguchi

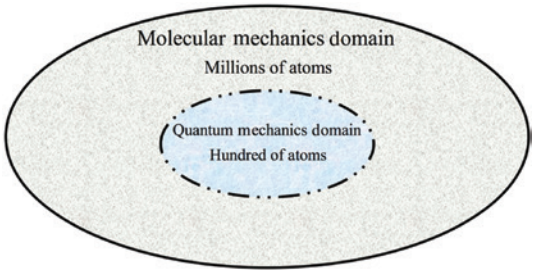

Figure 6: In hybrid QM/MM modeling, the MM domain encompasses the QM domain in a seamless fashion.

et al. (2011) and Zhong et al. (2000), the cohesive energy of grain boundaries was studied, Itakura et al. (2013) focused on assessing the effect of hydrogen on the mobility of a screw dislocation in bcc Fe using first-principles approach. Counts et al. (2010, 2011) provide a series of DFT computations to investigate the interaction of single and multiple H atoms in a body-centered cubic (bcc) Fe. They show that H-H interactions are weak as well as their maximum binding energy, while they investigate the binding energy of H to defects.

Similarly, Desai et al. (2010) studied the mechanistic aspects of hydrogen trapping in a Fe-Y alloy, using first-principles approach. Extending the work performed by the aforementioned authors, Matsumoto et al. (2014) performed MM simulations involving crack growth, nanoindentation, and tensile loading of a poly crystalline nanorod. They showed that in the case of crack growth and incorporating pseudo-hydrogen effects, the steels exhibited brittle behavior in nanoindentation simulations. Again, incorporating hydrogen pseudo-effects, the mechanism that was identified to be in play was HELP, and lastly, for tensile loading simulations, incorporating hydrogen pseudo-effects, the specimen fractured along the grain boundaries.

One of the most cited work regarding first-principles computation of fracture energy of Fe and Al due to hydrogen uptake is that of Jiang and Carter (2010) and Horstemeyer (2009). The authors assessed the ideal fracture energies of iron and aluminum in the presence of varying amounts of hydrogen, along with providing some insight into the cohesion-reduction mechanism of HE in metals. This work has been the foundation of many later works (Tadmor et al., 1996; Olden et al., 2008a,b, 2009a,b; Alvaro et al., 2014), which develop a macro-model, incorporating the results produced by Horstemeyer (2009).

Many times, *ab initio* calculations or QM/MMs are correlated with *in situ* testing and observation to validate the results produced by the multiscale computations in the lower scales. Tests like *in situ* transmission electron microscopy (TEM), where tests can be performed and observed at the nanoscale (dislocations, atoms, etc.), electrochemical nanoindentation, micropillar compression testing, which offers the possibility of quantifying the slip behavior of both single grains and grain boundaries, etc. They all can be correlated to diffusion and trapping parameters using an electrochemical permeation cell and a thermal desorption spectroscopy (TDS) system, respectively.

The *ab initio* and MM methods are well suited for studying phenomena at the nanoscale. It is very hard to link all the scales from QM scale to macroscale, so there is a real need to extend these methods to account for equipment scale engineering problems and structures.

4.2 Quasi-continuum density functional theory

A successful concurrent multiscale method that can address the phenomena that occur at the atomic scale with the accuracy of DFT and at the same time tackle length scales relevant to real-size structures or specimen testing is the quasi-continuum density functional theory, or simply QC, which was originally proposed by Tadmor et al. (Lu et al., 2006). The QC method combines atomistic methods with continuum models, which, compared to standalone atomistic or continuum simulations, offer great advantages in terms of computational efficiency and accuracy. The concept behind the QC method is that the processes that occur in the atomic level often occur in a very small domain, while the behavior of the rest of the atoms in the bulk of the steel can be modeled using well-established continuum theories. This underlying concept is exploited in the QC method by using atomistic modeling in the areas of interest while modeling the rest of the steel using continuum FE description. The present QC-DFT approach (Fivel, 2008; Peng et al., 2008; Peng & Lu, 2011) employs the combined QM and MM treatment, which was previously discussed and exhibited remarkable adaptability to changing circumstances, such as nucleation of new defects or migration of existing ones.

4.3 Discrete dislocation dynamics

While MM or MD methods can be employed to study one or a few dislocation lines and their interaction with other phenomena, e.g. hydrogen, the scale of the domain is small and MD is mostly used to study the properties of the dislocations in a model with volume not greater than 200 nm^3 (Devincre et al., 1992). Many times, there is a need to study a representative number of dislocations present in crystal and their interaction to derive useful conclusions regarding, e.g. dislocation mobility during plastic deformation, dislocation mobility with hydrogen residing in the dislocations, etc. Discrete dislocation dynamics (DDD) can tackle these problems by treating each dislocation explicitly and having elastic properties embedded in a crystal with elastic properties. External loadings are passed on to the dislocations through the crystal they are embedded in. In this sense, length scales up to 50 μm^3 can be simulated using DDD and a large number of

dislocations and their interaction can be modeled (Devincre et al., 1992). At higher length scales, CM models are used to solve the engineering problem, while DDD simulations are used to feed constitutive equations to the CM models. Three-dimensional discrete dislocation dynamics is the brain child of Kubin and Canova (1992) and Li (1964). The first example dealt with an fcc single crystal containing sets of edge and screw dislocations segments in a continuum media. Each finite dislocation segment generates a long-range elastic stress field, which, for the case of isotropic elasticity, was evaluated following the works of Li (De Wit, 1967) and De Wit (Willis, 1970). When anisotropy is at play, the line integrals proposed by Willis (Jothi et al., 2015a,b,c) are used. In this framework, the stress applied at each dislocation is effectively considered at the middle point of each segment. This stress is evaluated as the superposition of the internal stress by all other segments in the modeled 3D volume and the applied stress induced by the external loading. In fact, this induces a force that is expressed by the Peach-Koehler equation. DDD simulations can offer statistical data regarding dislocation densities, cumulated shear strain, stored energy, etc. (Devincre et al., 1992).

4.4 Microscale to macroscale modeling

A more computationally efficient approach, which many times is used in polycrystalline steels, e.g. steels, Al alloys, etc., is the coupling of a microscale model, with length scales comparable to the grain size of the studied steels (from a few to hundreds of micrometers) and the component size macroscale model. At the microscale, a polycrystalline unit cell, or representative volume element (RVE), is modeled, which contains grains and grain boundaries as well as other potential features such as crack, defects, voids, etc. (Benedetti & Aliabadi, 2015) (Figure 5). RVE can play a two-fold role. Either it can be used to determine the steel properties at the macro scale or it can be used to model the region of interest, e.g. a propagating crack, where the phenomena can be modeled at the microscale. The coupling of the two scales can be achieved, e.g. by transferring macro strains to the RVE as periodic boundary conditions while transferring the averaged micro stresses as macro stresses (Groeber et al., 2006). Another important feature of this method is the fact that both models are relatively easy to construct; the macro model mostly from CAD models or drawings of the specimens, and the microscale model can be constructed using a Dual-beam focused ion beam scanning electron microscope (FIB/SEM) combined with an electron backscatter diffraction (EBSD) system (Jothi et al., 2014a,b). Several works have focused on hydrogen-related phenomena, using the aforementioned method, such as the works of API 579-1 (2007), Rimoli and Ortiz (2010), Ebihara et al. (2011), Jothi et al. (2014a,b, 2015a,b,c), and Benedetti and Aliabadi (2015).

5 Typical case study from the O&G industry

In this section, a typical case study of HIC encountered in gas oil separation plants (GOSP) is described. Such plants are meant to treat the crude oil (a mixture of gas, oil, and unwanted components such as water, sand, and salts) extracted from the wells before being routed to downstream processes for further treatments (gas plants and refineries). In the GOSP, crude oil goes through a series of treatments taking place in carbon steel vessels such as gravity separators, desalters, and dehydrators, all connected through a complex network of piping systems. Due to the aggressive environment (wet sour hydrocarbons with relatively high level of H_2S partial pressure), such carbon steel equipment is prone to sour corrosion and HE degradation. Corrosion is mitigated/controlled through a comprehensive corrosion management program including the injection of corrosion inhibitors and the use of cathodic protection systems, lining, and internal coatings, as well as frequent inspection and monitoring. In addition, in order to mitigate sour service cracking (HIC), the metallurgy of the steel (and therefore the manufacturing process) is carefully selected at the design stage. Recall that since the late 1980s and the publication of the NACE standard TM0284 (HIC qualification test), steel selection for new equipment operating wet sour service applications is done in accordance with the NACE TM0284 standard and needs to meet the acceptance criteria given in NACE MR 0175/ISO 15156. This has put stringent pressure on the steel manufacturing industry to develop HIC-resistant steels (improved manufacturing process, low level of sulfur and impurities, and controlled shape of nonmetallic inclusions), which are now commonly used by the O&G industry.

The equipment of interest to this study is a carbon steel gravity separator referred to as high pressure production trap, or HPPT. The equipment was commissioned in 1973 (i.e. before the publication of NACE TM0284 standard) and is and made from ASTM A516 pressure vessel steel with an HIC-sensitive microstructure (hot rolled plates with high level of impurities, such as manganese sulfide inclusions,

Table 3: Relevant specifications of the HIC affected vessel considered in this study.

Service	Material	Nominal thickness	Operating pressure	Operating temperature	H_2S mol fraction	Calculated pH
Sour crude	ASTM A516	30.7 mm	120 psig	85 F	0.95%	5.6

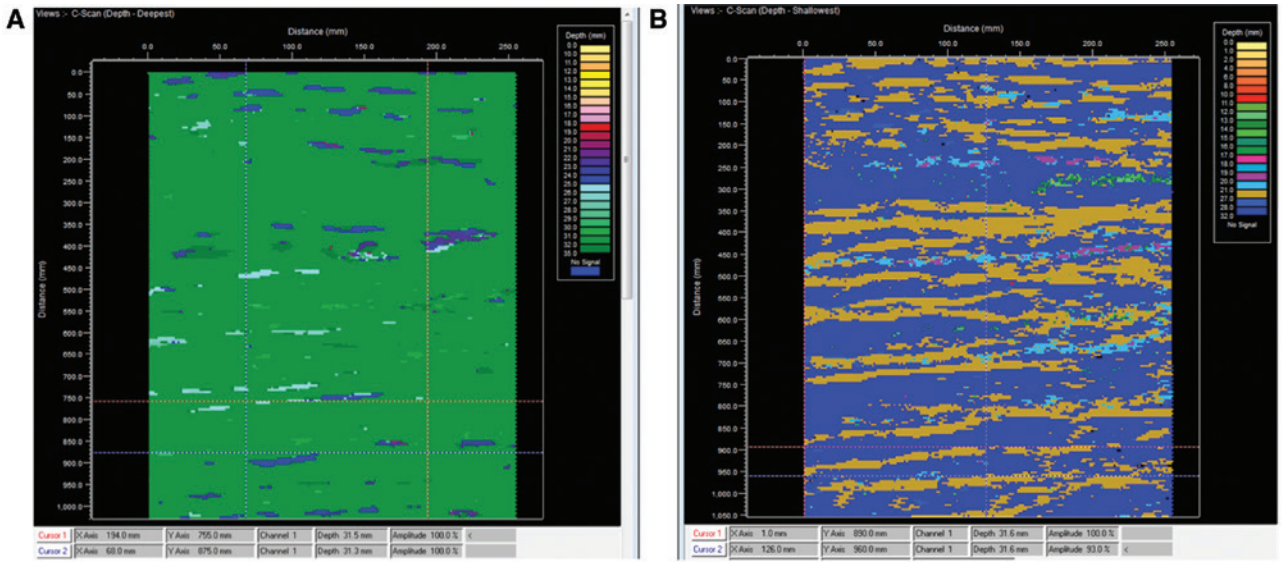

Figure 7: Ultrasonic C-SCAN imaging of an HIC affected location of the HPPT pressure vessel using a normal beam ultrasonic scanner. The scan dimensions are 255 mm in the horizontal/longitudinal direction and 1430 mm in the vertical/circumferential direction, with a resolution (step) of 5 mm in the vertical direction and 1 mm in the horizontal direction. Panel (A) represents the damage level in 2011, and its evolution in 2015 is shown in (B). Note that the color scale is inverted between (A) and (B).

MnS, commonly known to be preferential sites for HIC initiation). Table 3 summarizes some specifications of the vessel that are relevant to this study.

During NDT inspections, the vessel was found to suffer from different forms of HIC [with the presence of interconnected HIC in the form of step-wise cracking (SWC)]. Figure 7A shows a typical ultrasonic C-SCAN collected in 2011 on a damaged area of the vessel using a normal beam (0°) ultrasonic scanner. The contrast shows the position of the HIC damage in the through-thickness direction. Figure 7B shows a similar reading acquired on the same location after a 4-year period (2015), where the growth of the HIC damage in both longitudinal and circumferential directions is clearly visible. Note that such damage growth was initially mitigated/limited by internally coating the entire vessel with an epoxy-based coating to prevent corrosion (and therefore further hydrogen uptake); however, the evolution of damage presented in Figure 7 clearly indicates a significant coating degradation in this specific location of the vessel. In order to get some quantitative data on HIC growth rate, 20 randomly selected defects were manually analyzed and the distribution of the damage growth rate in both directions is presented in Figure 8.

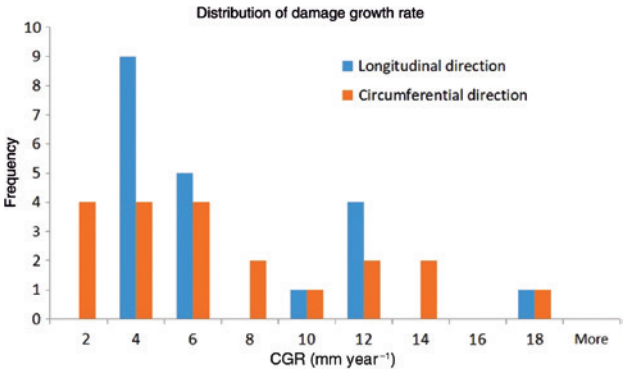

Figure 8: Distribution of field-measured linear HIC growth rates using 20 randomly selected defects. Note that the accuracy in the circumferential direction is ±5 mm due to the step size of the scanner in this direction.

The integrity of the vessel to fit for service was validated using a level 2 assessment following API-579 FFS standard. The main difficulty faced was to predict the remaining lifetime of the vessel before retirement, which is yet to be considered. Indeed, as highlighted in the API-579 standard, section 7.5.1: “At the present time,

there is no widely accepted method to predict the growth rate of active HIC or SOHIC damage; therefore, a standard method to assess the remaining life of a damaged structure cannot be established". There are numerous technical challenges that prevent the transfer of laboratory-based growth rate models to real industrial cases, which are covered in details in Section 6. Far from providing a "solution" to the study case presented in this section, the aim here is to share some relevant field data that might allow the scientific community to further investigate this type of damage.

6 Main challenges for transferability to industry

The oil industry has always been interested in long-term use of carbon steels, as they constitute the bulk steel used in pipelines, plant vessels, and piping systems. Nowadays, with increasing sourness of produced oil and gas, the development of large-scale lifetime prediction tools for aging equipment suffering from HE is of high interest to the oil and gas industry. This mainly consists of coupling existing HAC growth rate models to available best practices and standards for fitness for service such as ASME B31G (1991), British Standard-7910 (British Standard-2005), and API-579 (2007), in view of determining the remaining lifetime. The latter corresponds to the time necessary for the crack(s) to grow to a critical size, which would break the fitness for service criteria. Although HAC models are gaining increasing credibility in the industry due to their improved accuracy and complexity over the last decades, their integration into large-scale lifetime prediction software is still hindered by lots of persisting challenges. They are mainly related to (1) the difficulty in identifying boundary conditions and model parameters and (2) the complexity of actual field cases, which could break down the validity of the fracture mechanics similitude. Both aspects are discussed in more details in the following.

6.1 Model parameter identification

6.1.1 Microstructure and steel composition

One of the main sites of hydrogen trapping is the inclusion and segregation at the grain boundaries. For most carbon steels used in the oil and gas industry, large inclusions and metalloid segregation are present, which increases their susceptibility to HAC. Beyond the difficulty (or even impossibility) to characterize the statistics of such microstructural defects in carbon steel equipment under operation, multiscale statistical HAC models accounting for the non-uniform distribution of inclusions are still at infancy stage.

6.1.2 Defect sizing – non-destructive testing (NDT)

Defect detection and sizing is another major element in lifetime prediction of oil and gas assets. This relies on sound and accurate NDT techniques. Currently, the most widely used method for pipeline inspection is magnetic flux leakage in-line inspection (MFL-ILI), which is the basis for assessing the integrity of pipeline networks. The most accurate tools can reach an accuracy of ±10% of the wall thickness. Although MFL can detect loss of steels and features, which have a discontinuous structure, it shows very limited capabilities in detecting thin axial or narrow cracks, such as SCC. For embedded cracks, such as HIC, MFL usually fails to differentiate between a single HIC and cluster of HICs, usually reported as "laminations". Specifically, in NACE SP0102-2010, it is stated that for in-line inspection tools, the detection capability of common high-resolution MFL is very poor when it comes to fatigue cracking, SCC, long seam cracks, circumferential cracking, and cracks due to HIC. The situation is slightly improved when it comes to transverse MFL, with limited detection capabilities for SCC and fatigue cracks but still very poor detection for circumferential cracks and HIC cracks. Crack sizing capability is even beyond hope. The emergence of ultrasonic transducer-based pigs (UT-ILI), specifically developed for crack detection, showed promising results when it comes to crack detection, but sizing capabilities are still to be improved for the results to be used in lifetime prediction simulations.

The ultimate solution remains the advanced phased array UT (PAUT), which is commonly used for accurate sizing of defects in plant equipment (pressure vessels and piping systems) as well as during dig excavations on pipelines. Although PAUT can perfectly detect and size most types of HACs, the technique suffers from the limitation of being mostly manual (very costly for scanning large areas) and the quality of the results and interpretations is very much sensitive to the experience of the inspector.

Alternatively, acoustic emission (AE) is the technique showing promising results for detecting the onset and propagation of cracks whether they are circumferential, step wise, or SCC. AEs are stress waves produced from

sudden changes in internal stress distribution in steels caused by the changes in its internal structure. Possible causes for these internal structural changes in steels are crack initiation and growth, crack opening and closure, dislocation movement, etc. AE can readily detect the onset and the growth of the cracks in real time. Furthermore, with correct placement of the piezoelectric transducers, AE can detect the exact location of the cracks but AE cannot quantify the size of the cracks. A good approach then is to combine both methods, AE and PAUT, to simultaneously detect and quantify cracks evolving in oil and gas pipelines.

Although AE has been around for a long time already, it has not seen yet commercial uptake due to the following reasons

(a) AE produces large amounts of data and requires relatively sophisticated filtering analysis;
(b) AE reliability and accuracy in detecting small leaks are low; and
(c) AE results interpretation is highly dependent on skill, training, and expertise of personnel (Hydrosteel 6000, 2008).

Nevertheless, recent studies indicate that AE is gradually proving its reliability as an early detection method for cracks on pipelines. Consequently, further applications of AE are foreseen in the future once combined with PAUT (NACE 3T199, 1999).

6.1.3 Hydrogen charging conditions

Hydrogen charging is the main ingredient for subcritical cracking, and therefore, accurate knowledge of the hydrogen charging conditions is crucial to make accurate predictions of HE embrittlement HAC growth rates. Unlike simulated laboratory experiments, where the hydrogen charging conditions can be precisely determined and controlled (either by adjusting the electric current in electrochemical charging tests or by adjusting the test pressure in gaseous charging tests), hydrogen charging in real field conditions is not uniform in time and space and fluctuates throughout the lifetime of the equipment. A specific issue relevant to sour cracking in the O&G industry is related to the formation of passive iron sulfide film FeS on the steel surface during the corrosion process, which tends to limit/decrease the corrosion rate and the hydrogen permeation rate. Any upset in the operating conditions (e.g. change in pH, mechanical/chemical cleaning) could break the surface passivation and induce an increase in the permeation rate. As a result, the conditions on the hydrogen charging surface cannot be considered as uniform in space or constant with time. Another important difficulty in real field study cases is the potential presence of internal/external coatings meant to mitigate the sour corrosion from taking place and therefore the subsequent cracking. Such coatings tend to degrade with time, therefore allowing for wet sour H_2S to permeate through the coating and trigger the corrosion/cracking process again on the fresh steel surface. The lack of precise knowledge on the time degradation of such coatings makes it difficult to predict the time evolution of the hydrogen permeation rate to be used as input for crack grow models. The recommended alternative is the real-time measurement of the permeation flux on the equipment through its lifetime. Such exercise requires not only access to the equipment of interest (e.g. difficult for buried pipelines) but also availability of devices for reliable non-destructive hydrogen permeation rate measurements. Apart from the Hydrosteel probe (Smith et al., 2003), most other available devices as summarized in NACE 1C184 (2008) are laboratory prototypes with no proven success records in the field. The popularity of Hydrosteel is essentially related to its capacity to measure the *in situ* permeation rate with minimum (to no) surface preparation. In addition, its reliability is supported by published success records in field applications (Tems et al., 2002) as well as good agreement with standard electrochemical measurements carried out on laboratory specimens (Bosch et al., 2014). Assuming a Fickian diffusion and knowing the value of the hydrogen diffusivity of the equipment material, Hydrosteel flux measurements can be used to compute the subsurface hydrogen charging concentration, which is eventually used as an input to HAC models. Note, however, that flux measurements shall be carried out in healthy (i.e. non-cracked) regions of the equipment near the cracked region of interest. This is particularly important when dealing with embedded cracks (such as HIC and blisters), which absorb most of the hydrogen diffusing from the corrosion surface (Koers et al., 1996; Traidia et al., 2012), therefore leaving a very small amount to diffuse to the probe attached to the external wall. Another concern is related to hard-to-reach surfaces, typically buried pipelines, where excavations are necessary, resulting in important financial costs. A proposed solution is to use a correlation (which is yet to be developed) between the corrosion rate and the hydrogen permeation rate for the specific steel and environment of interest. Such correlation could be used to estimate the (average) permeation flux from corrosion rate values, which can be easily derived from available in-line inspection (ILI) records.

6.1.4 Fracture toughness and cohesion properties

Fracture toughness properties such as K_{TH}, J, and/or CTOD values are the prevailing parameters that are used in codes and related models to predict crack behavior in steels due to hydrogen-related degradation phenomena. In pipeline engineering, we are referring to low carbon steels while current and future steels tend to be very low carbon steels (<0.1 C). Fracture toughness properties such as K_{TH} are degraded by as much as 50% in hydrogen gas of pressure of 35 MPa, as indicated by Marchi and Somerday (2012), for X42, X52, X65, X70, and X80 steel grades. The same holds for electrolytic hydrogen charging. Numerous publications portray the deleterious effect of hydrogen electrolytic charging on fracture toughness properties of pipeline steels. To that end, the models presented in Section 3.3 could be used, such as the work of Olden et al. (2007, 2008a,b, 2009a,b, 2012) Alvaro et al. (2014), and Ha et al. (2014). Using these models, the fracture toughness properties can be correlated to hydrogen concentration ahead of the crack tip, which in turn can be used to calibrate the cohesive properties of the CZM model.

To validate models for predicting hydrogen influence on fracture toughness properties and cracking, databases of hydrogen tests need to be created, containing information from a wide set of pipeline steels.

Extensive work exists on hydrogen effect on cracking and fracture toughness properties and a lot of methods for testing, but there is a need to categorize and create database for relevant tests on pipeline steel grades, which will portray the testing conditions, charging methods, fracture toughness parameters measured and compared, etc. To that end, only a few databases exist, such as SANDIA's database (Marchi & Someday, 2012), which only refer to hydrogen charging in pressurized hydrogen. The complications in developing databases for testing of pipeline steels in hydrogen environments for use in validating relevant models are becoming complicated when we consider the number of tests that exist in the literature, hydrogen charging conditions, loading rate, *in situ* or *ex situ* hydrogen charging, etc. Furthermore, the classification of pipeline steels itself is also an issue, as pipeline steels are classified according to their yield strength (X65, X70, etc.), and many times, same grades might have different microstructures, so different behaviors for the same hydrogen testing conditions.

Regarding modeling for hydrogen-related phenomena, fracture toughness properties can be used to calibrate the models if the right testing regime is in place and there is confidence in the data; nevertheless, there are a few hurdles that can also hinder the wider adoption of relevant models. First, the CZM models presented in Section 3.3 require the measurement of the hydrogen concentration in the bulk of the steel; second, initial crack length measurements must be accurate, which is not always straightforward with in-line MFL methods, as aforementioned; and lastly and most importantly, the models presented consider a predetermined path for the crack when using the CZM. The CZM considers that the crack will grow in a known predetermined path, which many times cannot be predetermined due to uncertainties, when complex loading schemes and crack direction exist.

6.1.5 Hydrogen diffusivity

Experimental evidence on the correlation between stage II subcritical crack growth rate and the effective hydrogen diffusion coefficient (D_{Heff}), as shown in Figure 2, suggests that knowledge of D_{Heff} is a key input to lifetime prediction of HAC-affected components. There is a proliferation of published data on D_{Heff} for a variety of steels, including most of the carbon steels used in the oil and gas industry. However, review of these data reveals a significant discrepancy between published values, even for the same steel grade (Olden et al., 2008a,b). For example, for X65 pipeline steel, reported values of apparent diffusivities range from 10^{-5} cm^2/s to 10^{-7} cm^2/s, which is a variation by two orders of magnitude. Such a large discrepancy can be explained by multiple factors such as the difference in steel microstructure, specimen thickness, surface preparation, and permeation test conditions. This large variability in published values is a major concern to the reliability of numerical predictions. Therefore, the most reliable solution would be to measure directly D_{Heff} on permeation coupons extracted from steel plates of the same metallurgy as the equipment of interest. This is often not possible especially for aging equipment, where the steel grade is barely known. Consequently, a non-destructive technique/probe (which is yet to be developed) for *in situ* measurement of D_{Heff} in steel equipment under operation is very much desired.

6.1.6 Residual stresses

There are few studies dealing with the effect of residual stresses on HE susceptibility of carbon steels used in oil and gas industries, and yet their damage needs to be described consistently to be able to predict appropriately their lifetime and eventually their replacement. Nevertheless, the susceptibility to HE of high-strength steels, especially when it is pre-strained at slow strain-rate during tensile tests and/or in the presence of residual stresses,

is well documented. In general, the impact of residual stresses on HAC is important at relatively low external applied load. Typical situations in the oil and gas industry are SCC or HIC cracks near welds locations. Due to the difficulty in predicting the behavior of such cracks, fitness-for-service standards, such as API-579 (2007), make use of a minimum distance between the cracks and the weld below which the component does not fit for service, and advanced FEM analysis is required. Although a non-uniform distribution of residual stresses around a propagating HAC can be easily introduced in the stress analysis, especially for cohesive zone-based models described in Section 3.3, two main issues are foreseen. First, residual stresses may impact the crack path and cracking mode and thus deviate from the usual mode I straight crack growth assumption often considered in most existing HAC models. Second, even if the previous difficulty might be overcome by using some advanced multi-mode 3D fracture mechanics tools such as FRANC3D (Wawrzynek et al., 2012) (HAC models are yet to be implemented in this code), estimating the residual stresses due to welding can be quite challenging, especially for old equipment where manufacturing data may not have been kept in the records.

6.1.7 Initial conditions

The use of HAC models to predict the growth rate of pre-existing cracks in industrial steel equipment can also be hindered by the difficulty to accurately determine the initial boundary conditions in terms of hydrogen concentration distribution. This issue is particularly of concern for embedded bulk cracks, such as HIC experienced in sour oil and gas environment, where the amount of hydrogen initially entrapped inside the crack cavities cannot be measured and can hardly be estimated numerically. The only alternative to this is to consider a zero-bulk hydrogen concentration as an initial condition for the simulation, which means that all the history of actual hydrogen uptake that occurred in the past is omitted. Note that this assumption will influence only the incubation time, i.e. the time to the onset of crack growth, but will not influence the crack growth rate (Krom et al., 1997; Traidia et al., 2012).

6.2 Limitations of fracture mechanics similitude (specimen versus structure)

6.2.1 Small cracks

For a given steel in each hydrogen environment, a unique correlation between subcritical crack growth rate and SIF is based on the fracture mechanics similitude (discussed in Section 1). The K-similitude, which ensures that equal stress intensities (or equivalently J) will have equal consequences, is at the basis of transferring experiments and model results on small-scale specimens to large industrial structures for remaining life predictions.

Similar to fatigue cracking (Ritchie & Suresh, 1983), the K-similitude has been shown to breakdown for subcritical cracking at relatively small crack sizes. Experimental results by Gangloff (1985) carried out on AISI 4130 stressed in NaCl solution have shown the crack size effect of the threshold stress intensity. The latter declines sharply at crack sizes below 1 mm, which has been attributed to a local change in electrochemistry, which resulted in a tenfold increase of produced hydrogen at the crack surface. The breakdown of K-similitude for HAC at relatively small crack sizes remains quite poorly documented and deserves more attention for future research.

6.2.2 Load dynamics – *dK/dt* hydrogen charging conditions

In SCC and other hydrogen-related field cases, loading dynamics are relatively important. In particular, the loading scheme plays a significant role when dealing with practical field cases where load dynamics can become important due to the process conditions. For instance, there is close correlation between loading rate and hydrogen damage on fracture toughness properties of a cracked steel in a hydrogen environment (Bahrami et al., 2011; Chatzidouros et al., 2014). Furthermore, there is a subcritical cracking threshold for the crack initiation and for the crack arrest for given steels under hydrogen charging conditions, depending on the type of loading, i.e. constant displacement versus rising displacement (Nibur et al., 2013). Indeed, when constant displacement is applied, the crack initiation threshold is higher than the crack arrest threshold. This crack arrest is in turn higher than the crack initiation threshold for rising displacement. In addition, the cracking threshold is dependent on the yield strength of the steel (high-strength versus low- or medium-strength steel) (Nibur et al., 2013); precisely, the differences in the aforementioned cracking thresholds measurements increase with the decrease of the steel yield strength. The magnitude of the difference between crack initiation and crack arrest under constant displacement increases as the ratio of the fracture strain to the yield strain increases, i.e. $\varepsilon_f H/\varepsilon_0$ (H means under hydrogen charging).

The K-similitude reached its limit and becomes non-valid when load dynamics is relatively important. This is

manifested by a (da/dt) versus K curve, which starts to show dependency on dK/dt (Gangloff, 2003a,b). This fact particularly raises concern when dealing with practical field cases where load dynamics can become important due to process conditions or upsets. Load dynamics play also a significant role when it comes to hydrogen effect on high-strength pipeline steels. In general, high-strength steels in hydrogen environment have higher fatigue crack growth (FCG) rates than high-strength steels in inert environment. Whether the hydrogen environment is pressurized gas or electrolytic charging, the results always exhibit higher FCG rates of high-strength steels compared to FCG rates of steels in inert atmospheres. Loading rate and load cycle frequency also play a role in terms of FCG rate and HE severity. For instance, in the case of an AISI 4340 grade steel, HE is more severe in lower loading rates (dK/dt) (Clark & Landes, 1976), a conclusion that can easily be generalized to most high-strength steels. Furthermore, regarding FCG, HE is more severe in lower load cycle frequencies (Walter & Chandler, 1976).

Given these issues, it can be easily understood that models should be tuned and calibrated considering many variables regarding FCG. Furthermore, most of the developed models and simulations are built assuming small-scale yielding and small displacement conditions, which very often is not the case for real-world problems for high-strength pipeline steels, making them quite challenging to be transferred to larger scales.

6.2.3 Multiple crack interaction

Prediction of structural integrity in the presence of multiple cracks is a major challenge even in the absence of hydrogen. The assumption of K as the only governing parameter breaks down for nearby cracks, which could coalesce due to strong stress field interactions at crack tips. Typical issues in the oil and gas industry are SCC and step-wise HIC (also referred to as SWC). Several tentatives were proposed in the literature to better understand and model the growth and coalescence of such cracks. For internally pressurized multiple cracks, such as SWC, some tentatives were proposed by Iino (1978) and Suárez et al. (2000) to understand the mechanisms and conditions at which two individual HICs will coalesce into SWC, but the state of the art is still far from proposing a unified model that could stimulate the growth of multiple pressurized HICs and failure through SWC – a possible area for future work. For SCC, the state of the art is by far more mature (mainly driven by research in the nuclear industry). We note the pioneering work by Parkins and co-workers (Parkins, 1980; Parkins & Singh, 1990; Leis & Parkins, 1998), as well as the recent probabilistic tool *SCCrack* (Gangloff, 2016), which assumes that fracture similitude still applies, and Monte-Carlo-based models (Tohgo et al., 2009; Suzuki et al., 2010).

Note that simulation of hydrogen diffusion in the presence of multiple bulk cracks is still not well documented. Single HIC growth simulations revealed that cracks located near the inner wall (hydrogen production surface) tend to grow at a faster rate, thus shielding the area located behind them from hydrogen.

7 Summary and conclusions

There has been significant advancement in modeling of hydrogen-related phenomena. Most of the work are focused in translating the hydrogen mechanisms and damages in constitutive equations, which in turn are fitted in modeling schemes using CM. There is also significant work performed during the last 20 years using multiscale modeling schemes that attempt to tackle the underlying physics of hydrogen interaction with steels. Although hydrogen mechanisms as described in Section 2 clearly show that hydrogen affects steel in the micro-nanoscale, e.g. interaction with voids, dislocations, segregates, etc., the use of multiscale schemes is still mostly an academic exercise due to the complexity of the problem and the robustness of the methods.

Modeling schemes performed in the continuum domain dealing with HE could be used for integrity assessment and prediction of remaining life of oil and gas steel equipment, provided as follows:

- Databases exist on hydrogen influence on steels used in oil and gas industry and in various testing conditions, e.g. different hydrogen charging conditions, testing arrangements and measured parameters, correlation of measured parameters to hydrogen content in the steel, etc. These databases should be correlated with microstructures as well as with the grade of steels and have relevance with the field measurements. These databases will be used to calibrate the existing models, which should be used for integrity assessment.
- Improve crack detection and crack size measurement through NDT
- Training of personnel in using the modeling schemes. There is a need for high-skilled engineers in integrity assessment where modeling for hydrogen degradation is concerned.

Lastly, simulation schemes should be developed based on new or already developed theories and constitutive equations, which allow for the crack to grow freely without a predetermined path.

Nomenclature

AIDE	adsorption-induced dislocation emission
AE	acoustic emission
CAD	computer-aided design
C_{CRIT}	critical local hydrogen concentration
$C_{\mathrm{H\text{-}FPZ}}$	local hydrogen concentration at the FPZ
C_L	lattice hydrogen concentration
CM	continuum mechanics
C_T	trapped hydrogen concentration
CTOD	crack-tip opening displacement
CZM	cohesive zone modeling
DDD	discrete dislocation dynamics
DFT	density functional theory
D_{Heff}	trapped hydrogen diffusivity
E^*	total energy
EAM	embedded-atom method
EBSD	electron back-scattered diffraction
FCG	fatigue crack growth
FEM	finite element method
FIB	focused ion beam
FM	fracture mechanics
FPZ	fracture process zone
HAC	hydrogen-assisted cracking
HE	hydrogen embrittlement
HEAC	hydrogen environment assisted cracking
HEDE	hydrogen-enhanced decohesion
HELP	hydrogen-enhanced localized plasticity
HIC	hydrogen-induced cracking
HPT	hydrogen pressure theory
IHAC	internal hydrogen-assisted cracking
ILI	in line inspection
K_{TH}	threshold stress intensity
LEFM	linear elastic fracture mechanics
MD	molecular dynamics
MFL-ILI	magnetic flux leakage – in-line inspection
MM	molecular mechanics
NDT	non-destructive testing
PAUT	phased array ultrasonic transducer
QM	quantum mechanics
QC	quasi-continuum
RVE	representative volume element
SWC	step-wise corrosion
SSC	sulfide stress cracking
SCC	stress corrosion cracking
SOHIC	stress-oriented hydrogen induced cracking
SIF	stress intensity factor
SIHF	stress-induced hydride formation
SEM	scanning electron microscope
TDS	thermal desorption spectroscopy
TSL	traction separation law
UT-ILI	ultrasonic transducer-in-line inspection

Key to symbols

x_c	critical distance
t_c	critical period
x_a	elementary crack advance
x_d	diffusion distance
δ	crack opening
δ_c	critical crack opening
σ^*	local cohesive stress
V_H	partial molar volume of hydrogen
σ_H	hydrostatic stress
σ_c^*	critical cohesive stress
ε_p	local cumulative plastic strain

References

Ahn DC, Sofronis P, Dodds RH. On hydrogen-induced plastic flow localization during void growth and coalescence. Int J Hydrogen Energy 2007a; 32: 3734–3742.

Ahn DC, Sofronis P, Dodds R. Modeling of hydrogen-assisted ductile crack propagation in metals and alloys. Int J Fract 2007b; 145: 135–157.

Akhurst K, Baker T. The threshold stress intensity for hydrogen-induced crack growth. Metall Mater Trans A 1981; 12: 1059–1070.

Alvaro A, Olden V, Akselsen OM. 3D Cohesive modelling of hydrogen embrittlement in the heat affected zone of an X70 pipeline steel – Part II. Int J Hydrogen Energy 2014; 39: 3528–3541.

Alvaro A, Thue Jensen I, Kheradmand N, Løvvik OM, Olden V. Hydrogen embrittlement in nickel, visited by first principles modeling, cohesive zone simulation and nanomechanical testing. Int J Hydrogen Energy 2015; 40: 16892–16900.

API 579-1. Fitness-For-Service. American Petroleum Institute 2007.

ASME B31G: Manual for determining the remaining strength of corroded pipelines: a supplement to ASME B31 code for pressure piping. Revision of ANSI/ASME B31G-1984. ASME 1991.

ASTM E1681-03. Standard test method for determining threshold stress intensity factor for environment-assisted cracking of metallic materials, ASTM 2003.

Bahrami A, Bourgeon A, Cheaitani M. Effects of strain rate and microstructure on fracture toughness of duplex stainless steels under hydrogen charging conditions in International Conference on Ocean. Offshore and Arctic Engineering OMAE Rotterdam The Netherlands: ASME, 2011.

Beachem CD. A new model for hydrogen-assisted cracking (hydrogen “embrittlement”). Metall Trans 1972; 3: 441–455.

Benedetti I, Aliabadi MH. Multiscale modeling of polycrystalline materials: a boundary element approach to material degradation and fracture. Comput Methods Appl Mech Eng 2015; 289: 429–453.

Bernstein N, Kermode JR, Csányi G. Hybrid atomistic simulation methods for materials systems. Reports Prog Phys 2009; 72: 26501.

Birnbaum HK, Sofronis P. Hydrogen-enhanced localized plasticity – a mechanism for hydrogen-related fracture. Mater Sci Eng A 1994; 176: 191–202.

Bosch C, Cassagne T, Smith V, Kittel J. Hydrogen induced cracking (HIC) assessment of low alloy steel linepipe for sour service application – full scale HIC testing. NACE paper 2014-3893, presented at CORROSION 2014, San Antonio, Texas, 2014.

BRITISH STANDARD-7910. Guide to methods fo assessing the acceptability of flaws in metallic structures, 2005.

Chateau JP, Delafosse D, Magnin T. Numerical simulations of hydrogen – dislocation interactions in fcc stainless steels.: part II: hydrogen effects on crack tip plasticity at a stress corrosion crack. Acta Mater 2002; 50: 1523–1538.

Chatzidouros EV, Papazoglou VJ, Pantelis DI. Hydrogen effect on a low carbon ferritic-bainitic pipeline steel. Int J Hydrogen Energy 2014; 39: 18498–18505.

Chen X, Gerberich WW. The kinetics and micromechanics of hydrogen assisted cracking in Fe-3 pct Si single crystals. Metall Trans A 1991; 22: 59–70.

Choly N, Lu G, E W, Kaxiras E. Multiscale simulations in simple metals: a density-functional-based methodology. Phys Rev B 2005; 71: 94101.

Clark WG, Landes JD. An evaluation of rising load KISCC testing, stress corrosion – new approaches. In: Craig HL, editor. ASTM STP 610. West Conshohocken: American Society for Testing and Materials, 1976: 108–127.

Counts WA, Wolverton C, Gibala R. First-principles energetics of hydrogen traps in α-Fe: point defects. Acta Mater 2010; 58: 4730–4741.

Counts W, Wolverton C, Gibala R. Binding of multiple H atoms to solute atoms in bcc Fe using first principles. Acta Mater 2011; 59: 5812–5820.

Crolet J-L. Analysis of the various processes downstream cathodic hydrogen charging, I: diffusion, laboratory permeation and measurement of hydrogen content and diffusion coefficient. Mat Tech 2016; 104: 205.

Dadfarnia M, Sofronis P, Somerday BP, Liu JB, Johnson DD, Robertson IM. Modeling issues on hydrogen-induced intergranular cracking under sustained load. Proc 2008 Int Hydrog Conf – Eff Hydrog Mater 2009: 613–621.

Dadfarnia M, Sofronis P, Somerday BP, Balch DK, Schembri P. Degradation models for hydrogen embrittlement. In: Gangloff R, Somerday B, editors. Gaseous hydrogen embrittlement of materials in energy technologies: mechanisms, modelling and future developments. Cambridge, UK: Elsevier Inc., 2012: 326–377.

Dadfarnia M, Somerday BP, Schembri PE, Sofronis P, Foulk JW, Nibur KA, Balch DK. On modeling hydrogen-induced crack propagation under sustained load. JOM 2014; 66: 1390–1398.

Desai SK, Neeraj T, Gordon PA. Atomistic mechanism of hydrogen trapping in bcc Fe–Y solid solution: a first principles study. Acta Mater 2010; 58: 5363–5369.

Devincre B, Pontikis V, Brechet Y, Canova G, Condat M, Kubin L. Three-dimensional simulations of plastic flow in crystals. In: Mareschal M, Holian BL, editors. Microsc simulations complex hydrodyn phenom. Boston, MA: Springer, 1992: 413–423.

De Wit R. Some relations for straight dislocations. Phys Status Solidi 1967; 20: 567–573.

Ebihara K, Itakura M, Yamaguchi M. Evaluation of stress and hydrogen concentration at grain boundary of steels using three-dimensional polycrystalline model (selected papers of the Joint International Conference of Supercomputing in Nuclear Applications and Monte Carlo: SNA + MC 2010). Prog Nucl Sci Technol 2011; 2: 38–43.

Ferreira PJ, Robertson IM, Birnbaum HK. Hydrogen effects on the interaction between dislocations. Acta Mater 1998; 46: 1749–1757.

Fivel M. Discrete dislocation dynamics: principles and recent applications. In: Cazacu O, editor. Multiscale modeling of heterogenous materials: from microstructure to macro-scale properties. London, UK: Wiley-ISTE, 2008.

Fukai Y. The metal-hydrogen system: basic bulk properties. Berlin, Germany: Springer Science & Business Media, 2006.

Gangloff RP. Crack size effects on the chemical driving force for aqueous corrosion fatigue. Metall Trans A 1985; 16: 953–969.

Gangloff RP. Critical issues in hydrogen assisted cracking of structural alloys. In: Moody NR et al., editor. Hydrogen effects on materials behavior and corrosion deformation interactions. Warrendale, PA: TMS, 2003a: 447–497.

Gangloff RP. Hydrogen assisted cracking of high strength alloys. In: Milne I, Ritchie RO, Karihaloo B, editors. New York, NY: Comp Struct Integr Elsevier Science, 2003b.

Gangloff RP. Critical issues in hydrogen assisted cracking of structural alloys. Environ Crack Mater 2008: 141–165.

Gangloff RP. Probabilistic fracture mechanics simulation of stress corrosion cracking using accelerated laboratory testing and multi-scale modeling. Corrosion 2016; 72: 62–880.

Gangloff RP, Somerday BP. Gaseous hydrogen embrittlement of materials in energy technologies: mechanisms, modelling and future developments. Cambridge, UK: Elsevier, 2012.

Gerberich WW. Modelling hydrogen induced damage mechanisms in metals. In: Gangloff R, Somerday B, editors. Gaseous hydrogen embrittlement of materials in energy technologies: mechanisms, modelling and future developments. Cambridge, UK: Elsevier Inc., 2012: 209–246.

Gerberich WW, Livne T, Chen X-F. In: Jones RH, Gerberich WW, editors. Modeling environmental effects on crack initiation and propagation. Warrendale, PA: The Minerals, Metals & Materials Society, 1986: 243–257.

Gerberich WW, Livne T, Chen XF, Kaczorowski M. Crack growth from internal hydrogen-temperature and microstructure effects in 4340 steel. Metall Trans A 1988; 19: 1319–1334.

Gerberich WW, Oriani RA, Lii M, Chen X, Foecke T. The necessity of both plasticity and brittleness in the fracture thresholds of iron. Phil Mag A 1991; 63: 363–376.

Gerberich WW, Marsh PG, Hoehn JW. Hydrogen induced cracking mechanisms–are there critical experiments. Hydrog Eff Mater 1996: 539–551.

Groeber MA, Haley BK, Uchic MD, Dimiduk DM, Ghosh S. 3D Reconstruction and characterization of polycrystalline microstructures using a FIB–SEM system. Mater Charact 2006; 57: 259–273.

Ha HM, Ai JH, Scully JR. Effects of prior cold work on hydrogen trapping and diffusion in API X-70 line pipe steel during electrochemical charging. Corrosion 2014; 70: 166–184.

Hall MM, Symons DM. Hydrogen assisted fracture model for low potential stress corrosion cracking of Ni-Cr-Fe alloys. In: Jones R, editor. Chemistry and electrochemistry of corrosion and stress corrosion cracking. Warrendale, PA: The Minerals, Metals & Materials Society, 2001: 447–466.

Hirth J. Effects of hydrogen on the properties of iron and steel. Metall Trans A 1980; 11: 861–890.

Hirth JP, Rice JR. On the thermodynamics of adsorption at interfaces as it influences decohesion. Metall Trans A 1980; 11: 1501–1511.

Horstemeyer M. Multiscale modeling: a review. New Jersey, USA: Springer Science + Business Media, 2009.
Huang H, Gerberich WW. Crack-tip dislocation emission arrangements for equilibrium – II. Comparisons to analytical and computer simulation models. Acta Metall Mater 1992; 40: 2873–2881.
Huang H, Gerberich WW. Quasi-equilibrium modeling of the toughness transition during semibrittle cleavage. Acta Metall Mater 1994; 42: 639–647.
Hydrosteel 6000. Hydrogen flux monitor. UK: Ion Science Ltd. (2008).
Iino M. The extension of hydrogen blister-crack array in linepipe steels. Metall Trans A 1978; 9: 1581–1590.
Itakura M, Kaburaki H, Yamaguchi M, Okita T. The effect of hydrogen atoms on the screw dislocation mobility in bcc iron: a first-principles study. Acta Mater 2013; 61: 6857–6867.
Jiang DE, Carter EA. First principles assessment of ideal fracture energies of materials with mobile impurities: implications for hydrogen embrittlement of metals. Acta Mater 2004; 52: 4801–4807.
Johnson DF, Carter EA. First-principles assessment of hydrogen absorption into FeAl and Fe3Si: towards prevention of steel embrittlement. Acta Mater 2010; 58: 638–648.
Jothi S, Croft TN, Brown SGR. Influence of grain boundary misorientation on hydrogen embrittlement in bi-crystal nickel. Int J Hydrogen Energy 2014a; 39: 20671–20688.
Jothi S, Croft TN, Brown SGR, De Souza Neto EA. Finite element microstructural homogenization techniques and intergranular intragranular microstructural effects on effective diffusion coefficient of heterogeneous polycrystalline composite media. Compos Struct 2014b; 108: 555–564.
Jothi S, Croft TN, Wright L, Turnbull A, Brown SGR. Multi-phase modelling of intergranular hydrogen segregation/trapping for hydrogen embrittlement. Int J Hydrogen Energy 2015a; 40: 15105–15123.
Jothi S, Croft TN, Brown SGR. Coupled macroscale-microscale model for hydrogen embrittlement in polycrystalline materials. Int J Hydrogen Energy 2015b; 40: 2882–2889.
Jothi S, Croft TN, Brown SGR. Multiscale multiphysics model for hydrogen embrittlement in polycrystalline nickel. J Alloys Compd Suppl 2015c; 645: 500–504.
Jouiad M, Clement N, Coujou A. Friction stresses in the γ phase of a nickel-based superalloy. Phil Mag A 1998; 77: 689–699.
Kirchheim R. Hydrogen solubility and diffusivity in defective and amorphous metals. Prog Mater Sci 1988; 32: 261–325.
Koers RWJ, Krom AHM, Bakker A. Modelling hydrogen induced cracking using a coupled diffusion-elasto-plastic stress analysis. Poitiers, France: ECF11 Poitiers, 1996.
Kohn W, Sham LJ. Self-consistent equations including exchange and correlation effects. Phys Rev 1965; 140: A1133–A1138.
Krom AHM, Bakker A, Koers RWJ. Modelling hydrogen-induced cracking in steel using a coupled diffusion stress finite element analysis. Int J Press Vessel Pip 1997; 72: 139–147.
Krom AHM, Koers RWJ, Bakker A. Hydrogen transport near a blunting crack tip. J Mech Phys Solids 1999; 47: 971–992.
Kubin L, Canova G. The modelling of dislocation patterns. Scr Metall Mater 1992; 27: 957–962.
Kumnick AJ, Johnson HH. Deep trapping states for hydrogen in deformed iron. Acta Materialia 1980; 28: 33–39.
Lee SL, Unger DJ. A decohesion model of hydrogen assisted cracking. Eng Fract Mech 1988; 31: 647–660.
Leis BN, Parkins RN. Mechanics and material aspects in predicting serviceability limited by stress-corrosion cracking. Fatigue Fract Eng Mater Struct 1998; 21: 583–601.
Li JCM. Stress field of a dislocation segment. Phil Mag 1964; 10: 1097–1098.
Liang Y, Sofronis P. Toward a phenomenological description of hydrogen-induced decohesion at particle/matrix interfaces. J Mech Phys Solids 2003; 51: 1509–1531.
Liang Y, Sofronis P. On hydrogen-induced void nucleation and grain boundary decohesion in nickel-base alloys. J Eng Mater Technol 2004; 126: 368–377.
Liang Y, Sofronis P, Dodds RH. Interaction of hydrogen with crack-tip plasticity: effects of constraint on void growth. Mater Sci Eng A 2004; 366: 397–411.
Liang Y, Ahn DC, Sofronis P, Dodds RH, Bammann D. Effect of hydrogen trapping on void growth and coalescence in metals and alloys. Mech Mater 2008; 40: 115–132.
Lin H, Truhlar DG. QM/MM: what have we learned, where are we, and where do we go from here? Theor Chem Acc 2006; 117: 185–199.
Lu G, Kaxiras E. Handbook of theoretical and computational nanotechnology. Stevenson Ranch, CA: American Scientific, 2004.
Lu G, Kaxiras E. Hydrogen embrittlement of aluminum: the crucial role of vacancies. Phys Rev Lett 2005; 94: 155501.
Lu G, Tadmor EB, Kaxiras E. From electrons to finite elements: a concurrent multiscale approach for metals. Phys Rev B 2006; 73: 24108.
Lynch SP. Mechanism of hydrogen assisted cracking – a review. In: Moody NR, Thompson AW, editors. Hydrogen effects in materials. Warrendale, PA: The Minerals, Metals and Materials Society, 2003.
Lynch SP. Hydrogen embrittlement phenomena and mechanisms. Corros Rev 2012; 30: 105–123.
Magnin T. Advances in corrosion-deformation interactions. Materials Science Forum 1995; 202.
Marchi CS, Somerday BP., Technical reference on hydrogen compatibility of materials: plain carbon ferritic steels: C–Mn alloys (Code 1100), Sandia. National Laboratories, 2012.
Matsumoto R, Seki S, Taketomi S, Miyazaki N. Hydrogen-related phenomena due to decreases in lattice defect energies – molecular dynamics simulations using the embedded atom method potential with pseudo-hydrogen effects. Comput Mater Sci 2014; 92: 362–371.
McLellan RB, Harkins CG. Hydrogen interactions with metals. Mater Sci Eng 1975; 18: 5–35.
Momida H, Asari Y, Nakamura Y, Tateyama Y, Ohno T. Hydrogen-enhanced vacancy embrittlement of grain boundaries in iron. Phys Rev B 2013; 88: 144107.
NACE International. Techniques for monitoring corrosion and related parameters in field applications. NACE International Publication 3T199, 1999.
NACE 1C184. Hydrogen permeation measurement and monitoring, 2008.
Needleman A. A continuum model for void nucleation by inclusion debonding. J Appl Mech 1987; 54: 525.
Neimitz A, Aifantis EC. On certain fracture mechanics considerations in environmental cracking. In: Krausz AS, Martinus Nijhoff, editors. Time dependent fracture. Dordrecht: Springer, 1985, 189–200.
Neimitz A, Aifantis EC. On the size and shape of the process zone. Eng Fract Mech 1987a; 26: 491–503.

Neimitz A, Aifantis EC. On the length of crack jump during subcritical growth. Eng Fract Mech 1987b; 26: 505–518.
Nibur KA, Somerday BP, Marchi CS, Foulk JW, Dadfarnia M, Sofronis P. The relationship between crack-tip strain and subcritical cracking thresholds for steels in high-pressure hydrogen gas. Metall Mater Trans A 2013; 44:248–269.
Olden V, Thaulow C, Johnsen R, Østby E. Cohesive zone modeling of hydrogen-induced stress cracking in 25% Cr duplex stainless steel. Scr Mater 2007; 57: 615–618.
Olden V, Thaulow C, Johnsen R. Modelling of hydrogen diffusion and hydrogen induced cracking in supermartensitic and duplex stainless steels. Mater Des 2008a; 29: 1934–1948.
Olden V, Thaulow C, Johnsen R, Østby E, Berstad T. Application of hydrogen influenced cohesive laws in the prediction of hydrogen induced stress cracking in 25% Cr duplex stainless steel. Eng Fract Mech 2008b; 75: 2333–2351.
Olden V, Thaulow C, Berstad T, Østby E. Prediction of hydrogen embrittlement in 25% Cr duplex stainless steel based on cohesive zone simulation. Proc Int Conf Offshore Mech Arct Eng – OMAE 2009a; 6: 209–218.
Olden V, Thaulow C, Johnsen R, Østby E, Berstad T. Influence of hydrogen from cathodic protection on the fracture susceptibility of 25%Cr duplex stainless steel – constant load SENT testing and FE-modelling using hydrogen influenced cohesive zone elements. Eng Fract Mech 2009b; 76: 827–844.
Olden V, Alvaro A, Akselsen OM. Hydrogen diffusion and hydrogen influenced critical stress intensity in an API X70 pipeline steel welded joint-experiments and FE simulations. Int J Hydrogen Energy 2012; 37: 11474–11486.
Oriani RA. A mechanistic theory of hydrogen embrittlement of steels. Berichte Der Bunsengesellschaft Für Phys Chem 1972; 76: 848–857.
Pardee WJ, Paton NE. Model of sustained load cracking by hydride growth in Ti alloys. Metall Trans A 1980; 11: 1391–1400.
Parkins RN. Predictive approaches to stress corrosion cracking failure. Corros Sci 1980; 20: 147–166.
Parkins RN, Singh PM. Stress corrosion crack coalescence. Corrosion 1990; 46: 485–499.
Peng Q, Lu G. A comparative study of fracture in Al: quantum mechanical vs. empirical atomistic description. J Mech Phys Solids 2011; 59: 775–786.
Peng Q, Zhang X, Hung L, Carter EA, Lu G. Quantum simulation of materials at micron scales and beyond. Phys Rev B 2008; 78: 54118.
Rice JR, Wang JS. Embrittlement of interfaces by solute segregation. Mater Sci Eng A 1989; 107: 23–40.
Rimoli JJ, Ortiz M. A three-dimensional multiscale model of intergranular hydrogen-assisted cracking. Phil Mag 2010; 90: 2939–2963.
Ritchie RO, Suresh S. The fracture mechanics similitude concept: questions concerning its application to the behavior of short fatigue cracks. Mater Sci Eng 1983; 57: 27–30.
Ritchie R, Knott J, Rice J. On the relationship between critical tensile stress and fracture toughness in mild steel. J Mech Phys Solids 1973; 21: 395–410.
Robertson IM. The effect of hydrogen on dislocation dynamics. Eng Fract Mech 2001; 68: 671–692.
Robertson IM, Birnbaum HK, Sofronis P. Hydrogen effects on plasticity. Dislocations Solids 2009; 15: 249–293.
Robertson IM, Sofronis P, Nagao A, Martin ML, Wang S, Gross DW, Nygren KE. Hydrogen embrittlement understood. Metall Mater Trans B 2015; 46: 1085–1103.
Schwalbe K. Discussion: "Finite element solutions of crack tip behavior in small scale yielding. J Eng Mater Technol 1977; 99: 186–187.
Serebrinsky A, Carter EA, Ortiz M. A quantum-mechanically informed continuum model of hydrogen embrittlement. J Mech Phys Solids 2004; 52: 2403–2430.
Sirois E, Birnbaum HK. Effects of hydrogen and carbon on thermally activated deformation in nickel. Acta Metall Mater 1992; 40: 1377–1385.
Smith VCM, Martin JW, Hinds G, Street N, Bosch C, Haase T, Jäger S. HIC resistance of heritage pipelines exposed to mildly sour environments. NACE International, 2003.
Sofronis P, Birnbaum HK. Mechanics of the hydrogen-dislocation-impurity interactions – I. Increasing shear modulus. J Mech Phys Sol 1995; 43: 49–90.
Sofronis P, McMeeking R. Numerical analysis of hydrogen transport near a blunting crack tip. J Mech Phys Solids 1989; 37: 317–350.
Sofronis P, Liang Y, Aravas N. Hydrogen induced shear localization of the plastic flow in metals and alloys. Eur J Mech A/Solids 2001; 20: 857–872.
Suárez VJC, Velázquez JLG, López JMH, Robles JGR. Finite element analysis of the interaction of hydrogen induced stepwise cracks. ECF13 San Sebastian 2000.
Suzuki H, Tohgo K, Shimamura Y, Nakayama G, Hirano T. Monte Carlo simulation of stress corrosion cracking on smooth surface of a sensitized stainless steel type 304 under non-uniform stress condition. J Solid Mech Mater Eng 2010; 4: 898–907.
Tadmor EB, Ortiz M, Phillips R. Quasicontinuum analysis of defects in solids. Philos Mag A 1996; 73: 1529–1563.
Taha A, Sofronis P. A micromechanics approach to the study of hydrogen transport and embrittlement. Eng Fract Mech 2001; 68: 803–837.
Tateyama Y, Ohno T. Stability and clusterization of hydrogen-vacancy complexes in a-Fe: an ab-initio study. Phys Rev B 2003; 67: 174105.
Tems RD, Lewis AL, Abdulhadi AI. Field and laboratory measurements with hydrogen permeation measurement devices. Denver, Colorado: NACE, 2002.
Tetelman AS. Fundamental aspects of stress corrosion cracking. Natl Assoc Corros Eng Houst 1969: 446.
Tohgo K, Suzuki H, Shimamura Y, Nakayama G, Hirano T. Monte Carlo simulation of stress corrosion cracking on a smooth surface of sensitized stainless steel type 304. Corros Sci 2009; 51: 2208–2217.
Toribio J, Kharin V. The effect of history on hydrogen assisted cracking: 1. coupling cf hydrogenation and crack growth. Int J Fract 1997; 88: 233–245.
Traidia A, Alfano M, Lubineau G, Duval S, Sherik A. An effective finite element model for the prediction of hydrogen induced cracking in steel pipelines. Int J Hydrogen Energy 2012; 37: 16214–16230.
Turnbull A, Ferriss DH, Anzai H. Modelling of the hydrogen distribution at a crack tip. Mater Sci Eng A 1996; 206: 1–13.
Unger DJ. On a decohesion model of hydrogen assisted cracking. In: Tenth US. Austin, TX: Natl Congr Appl Mech 1986.
Unger DJ. A mathematical analysis for impending hydrogen assisted crack propagation. Eng Fract Mech 1989; 34: 657–667.

Unger DJ. Analytical fracture mechanics edition. Elsevier, eBook ISBN: 9780080527192, 1995.

Van Leeuwen HP. Quantitative models of hydrogen-induced cracking in high strength steels. Rev Coatings Corros 1979; 4: 5–93.

Von Appen J, Dronskowski R, Chakrabarty A, Hickel T, Spatschek R, Neugebauer J. Impact of Mn on the solution enthalpy of hydrogen in austenitic Fe-Mn alloys: a first-principles study. J Comput Chem 2014; 35: 2239–2244.

Walter RJ, Chandler WT. Cyclic-load crack growth in ASME SA-105 grade II steel in high-pressure hydrogen at ambient temperature. Effect of Hydrogen on Behavior of Materials. In: Moran, WY: NASA Technical Report, 1976.

Wawrzynek P, Carter B, Ingraffea AR. Advances in simulation of arbitrary 3D crack growth using FRANC3D NG ICF12. Ottawa 2009; 2012: 1–11.

Willis JR. Stress fields produced by dislocations in anisotropic media. Phil Mag 1970; 21: 931–949.

Yamaguchi M, Ebihara KI, Itakura M, Kadoyoshi T, Suzudo T, Kaburaki H. First-principles study on the grain boundary embrittlement of metals by solute segregation: part II. Metal (Fe, Al, Cu)-Hydrogen (H) Systems. Metall Mater Trans A 2011; 42: 330–339.

Zapffe C, Sims C. Hydrogen embrittlement, internal stress and defects in steel. Trans AIME 1941; 1307: 1–37.

Zhang X, Zhao Y, Lu G. Recent development in quantum mechanics/molecular mechanics modeling for materials 2012; 10: 65–82.

Zhong L, Wu R, Freeman AJ, Olson GB. Charge transfer mechanism of hydrogen-induced intergranular embrittlement of iron. Phys Rev B 2000; 62: 13938–13941.